

Mathematical Modeling of the AEDC Propulsion Wind Tunnel (16T)

Philip B. Stich
Calspan Field Services, Inc.

Property of U. S. Air Force
AEDC LIBRARY
F40600-01-G-0004

March 1985

Final Report for Period 1 October 1978 — 30 September 1982

**TECHNICAL REPORTS
FILE COPY**

Approved for public release; distribution unlimited.

**ARNOLD ENGINEERING DEVELOPMENT CENTER
ARNOLD AIR FORCE STATION, TENNESSEE
AIR FORCE SYSTEMS COMMAND
UNITED STATES AIR FORCE**

AEDC TECHNICAL LIBRARY



5 0720 00035 1207

NOTICES

When U. S. Government drawings, specifications, or other data are used for any purpose other than a definitely related Government procurement operation, the Government thereby incurs no responsibility nor any obligation whatsoever, and the fact that the government may have formulated, furnished, or in any way supplied the said drawings, specifications, or other data, is not to be regarded by implication or otherwise, or in any manner licensing the holder or any other person or corporation, or conveying any rights or permission to manufacture, use, or sell any patented invention that may in any way be related thereto.

Qualified users may obtain copies of this report from the Defense Technical Information Center.

References to named commercial products in this report are not to be considered in any sense as an endorsement of the product by the United States Air Force or the Government.

This report has been reviewed by the Office of Public Affairs (PA) and is releasable to the National Technical Information Service (NTIS). At NTIS, it will be available to the general public, including foreign nations.

APPROVAL STATEMENT

This report has been reviewed and approved.



RICHARD B. JAMER, Major, CF
Directorate of Technology
Deputy for Operations

Approved for publication:

FOR THE COMMANDER



MARION L. LASTER
Director of Technology
Deputy for Operations

UNCLASSIFIED

SECURITY CLASSIFICATION OF THIS PAGE

REPORT DOCUMENTATION PAGE

1a. REPORT SECURITY CLASSIFICATION Unclassified			1b. RESTRICTIVE MARKINGS		
2a. SECURITY CLASSIFICATION AUTHORITY			3. DISTRIBUTION/AVAILABILITY OF REPORT Approved for public release; distribution unlimited.		
2b. DECLASSIFICATION/DOWNGRADING SCHEDULE N/A			5. MONITORING ORGANIZATION REPORT NUMBER(S)		
4. PERFORMING ORGANIZATION REPORT NUMBER(S) AEDC-TR-84-32			7a. NAME OF MONITORING ORGANIZATION		
6a. NAME OF PERFORMING ORGANIZATION Arnold Engineering Development Center		6b. OFFICE SYMBOL (If applicable)	7b. ADDRESS (City, State and ZIP Code)		
6c. ADDRESS (City, State and ZIP Code) Arnold Air Force Station, TN 37389			9. PROCUREMENT INSTRUMENT IDENTIFICATION NUMBER		
8a. NAME OF FUNDING/SPONSORING ORGANIZATION		8b. OFFICE SYMBOL (If applicable)	10. SOURCE OF FUNDING NOS.		
8c. ADDRESS (City, State and ZIP Code)			PROGRAM ELEMENT NO.	PROJECT NO.	TASK NO.
11. TITLE (Include Security Classification) Mathematical Modeling of the AEDC			65807F	D216	WORK UNIT NO.
12. PERSONAL AUTHOR(S) Stich, Philip B., Calspan Field Services, Inc.					
13a. TYPE OF REPORT Final		13b. TIME COVERED FROM 781001 TO 820930		14. DATE OF REPORT (Yr., Mo., Day) 1985 March	
				15. PAGE COUNT 108	
16. SUPPLEMENTARY NOTATION Available in Defense Technical Information Center (DTIC).					
17. COSATI CODES			18. SUBJECT TERMS (Continue on reverse if necessary and identify by block number)		
FIELD	GROUP	SUB. GR.	mathematical models pressure flow		
12	01		transonic wind tunnel temperature		
14	02		computer program power		
19. ABSTRACT (Continue on reverse if necessary and identify by block number) An empirically based model of the 16-ft Propulsion Wind Tunnel (16T) at the Arnold Engineering Development Center (AEDC), has been developed for calculating the distribution of tunnel component pressure losses and the effect of changes in these pressure losses on the tunnel total-power requirements. The model consists of two separate computer programs. The Historical Program assesses tunnel performance from a historical data base which was acquired during prior tunnel operation. The Analytical Model uses component pressure-loss information calculated by the Historical Program to evaluate potential changes in tunnel component pressure losses with respect to the tunnel power. The model was used to assess the potential power savings for a modification to the Tunnel 16T diffuser, which involves the replacement of the compressor protective screen. Results indicate that for each 1-percent increase in diffuser recovery, a 4-percent decrease in main drive power will result. Less significant power savings were found for improvements to the other tunnel components.					
20. DISTRIBUTION/AVAILABILITY OF ABSTRACT UNCLASSIFIED/UNLIMITED <input type="checkbox"/> SAME AS RPT. <input checked="" type="checkbox"/> DTIC USERS <input type="checkbox"/>			21. ABSTRACT SECURITY CLASSIFICATION Unclassified		
22a. NAME OF RESPONSIBLE INDIVIDUAL W. O. Cole			22b. TELEPHONE NUMBER (Include Area Code) Ext. 615-455-2611, 7813		22c. OFFICE SYMBOL DOS

DD FORM 1473, 83 APR

EDITION OF 1 JAN 73 IS OBSOLETE.

UNCLASSIFIED

SECURITY CLASSIFICATION OF THIS PAGE

UNCLASSIFIED

SECURITY CLASSIFICATION OF THIS PAGE

Block 11. (Concluded)

Propulsion Wind Tunnel (16T). (U)

UNCLASSIFIED

SECURITY CLASSIFICATION OF THIS PAGE

PREFACE

The work reported herein was sponsored by the Arnold Engineering Development Center (AEDC), Air Force Systems Command (AFSC), Arnold Air Force Station, Tennessee under Contract No. F40600-81-C-003. The manuscript was submitted for publication on September 26, 1984.

The reproducibles used in the reproduction of this report were supplied by the author.

Acknowledgments

The author wishes to thank the United States Air Force and the officials of Calspan Field Services, Inc., for permission to use the results presented herein. The efforts of the late Leroy J. David, who initiated this work, are acknowledged and special appreciation expressed. Thanks are due to Mr. Frank Jackson, the author's supervisor, for his direction and encouragement in the work, and appreciation is expressed to Dr. Kenneth E. Harwell, who, assisted in the preparation and review of the thesis and to Dr. Frank G. Collins and Dr. Charles C. Limbaugh.

CONTENTS

	<u>Page</u>
1.0 INTRODUCTION	9
1.1 Statement of Problem	9
1.2 Objective	11
2.0 TEST FACILITY	13
2.1 General	13
2.2 Tunnel Components, Geometry, and Support Systems	13
3.0 ANALYTICAL APPROACH	31
3.1 General	31
3.2 Tunnel Component Model	32
3.3 Flow Equations	34
3.4 Compressor Relationships	40
3.5 Main Drive System Model	42
3.6 Thermodynamic Relationships	45
3.7 Plenum Evacuation System Model	52
4.0 MODELING PROCEDURE	61
4.1 Historical Program	61
4.2 Analytical Model	64
5.0 RESULTS AND DISCUSSION	70
5.1 General	70
5.2 Historical Program	70
5.3 Analytical Model	80
6.0 CONCLUSIONS AND RECOMMENDATIONS	97
REFERENCES	99

ILLUSTRATIONS

<u>Figure</u>	<u>Page</u>
1. Operating Regime for Tunnel 16T	14
2. Components and Dimensions for Tunnel 16T	15
3. Compressor C1 Layout for Tunnel 16T (Ref. 6), . . .	19
4. Compressor C1 Performance Map	20
5. Flexible Nozzle for Tunnel 16T	23
6. Diffuser for Tunnel 16T	26
7. Schematic View of Plenum Evacuation System . . .	29
8. Component Model of Tunnel 16T	33
9. Main Drive Motor Efficiency	44
10. Main Drive System Efficiency	46
11. Total Temperature-Entropy Diagram for Tunnel 16T Model	47
12. Performance Characteristics of Plenum Evacuation System First- and Second-Stage Compressors for an Inlet Temperature of 100°F	54
13. PES Pressure Control Staging Regimes in Tunnel 16T	57
14. Historical Program Flow Chart	62
15. Tunnel Component Pressure-Loss Coefficients with Curvefits and Curvefit Coefficients	66

<u>Figure</u>	<u>Page</u>
16. Historical Program Tunnel Performance Plots . . .	66
17. Analytical Model Flow Chart	68
18. Test Conditions for Historical Program Data Sets	71
19. Calculated Tunnel Component Loss Coefficients	74
20. Percentage of Power Dissipation for Tunnel Components	76
21. Main Drive Power Levels for Historical Program Data Sets	81
22. Effect of Variation of Test Section Pressure-Loss Coefficient on Main Drive Power	87
23. Effect of Variation of Diffuser Pressure-Loss Coefficient on Main Drive Power	88
24. Effect of Variation of Corner 1 Pressure-Loss Coefficient on Main Drive Power	90
25. Effect of Variation of Backleg Pressure-Loss Coefficient on Main Drive Power	91

<u>Figure</u>	<u>Page</u>
26. Effect of Variation of Compressor Efficiency on Main Drive Power	92
27. Effect of a 2.5-percent Increase in Diffuser Recovery on Main Drive Power	94
28. Historical Distribution of Air-On Test Time at Various Mach Numbers in Tunnel 16T	95

TABLES

1. Seasonal Cooling Water Temperatures (Ref. 4) .	22
2. PES Pressure Control Staging Regimes	56
3. PES Pressure Control Compressor Configurations.	56
4. PES Compressor Pressure Ratios for Multiple Stage Configurations	58
5. Power Dissipation Values for Tunnel Components Historical Program and Analytical Model	82
6. Comparison of Historical Program and Analytical Model PES Power and Configurations	84

APPENDICES

	<u>Page</u>
A. DERIVATION OF FAN-LAW CORRECTIONS FOR COMPRESSOR C1	101
B. DERIVATION OF ADIABATIC EFFICIENCY EQUATION FOR A POLYTROPIC COMPRESSION	104
NOMENCLATURE	106

1.0 INTRODUCTION

1.1 Statement of Problem

The rapidly increasing price of electrical energy is the primary factor leading to the growing cost of wind tunnel testing over the last ten years. The rise in cost has precipitated intensive efforts to reduce the power consumption of the wind tunnels at the Arnold Engineering Development Center (AEDC). Of primary concern is the 16-ft Transonic Wind Tunnel (16T) in the Propulsion Wind Tunnel Facility (PWT) which is the largest single consumer of electrical energy at AEDC.

In general terms, a closed-circuit wind tunnel is a relatively simple thermodynamic machine composed of ducting and other components which have energy (or pressure) losses caused by friction, flow direction and velocity changes, and thermodynamic inefficiencies. The combination of the energy losses for a particular test facility geometry (and set of test conditions) determines the compressor input shaft power requirements and hence is a primary part of the operational expenses of the test facility. An accurate determination of the ducting

pressure losses is therefore a very essential step in the design of an efficient wind tunnel facility.

Numerous individuals have made significant contributions to the calculation of ducting pressure losses and analysis of wind tunnel losses. Wattendorf laid the foundation for the analysis of wind tunnel losses in his 1938 publication (Ref. 1). A compilation of wind tunnel component loss data for subsonic flow was published in 1950 by J. Don Gray of ARO, Inc. Another significant collection of loss data was published by the Society of Automotive Engineers (SAE) in 1962 (Ref. 2). In 1968, a computer program was developed by J. A. Gunn, E. M. Kraft, and M. W. Poole of ARO, Inc., for calculating ducting system pressure losses. Documentation of this program also contained a compilation of loss formulae especially pertinent for wind tunnel applications. An interactive computer program for evaluating the performance of wind tunnel test facilities based entirely on geometric inputs was developed by Jackson in 1976. The documentation of this program (Ref. 3) contains an excellent compilation of data and duct loss formulae.

Efforts to reduce the Tunnel 16T pressure losses, and consequently the energy consumption, primarily involve the geometric modification of tunnel ducting and/or

components within the tunnel ducting. Before implementation of such modifications can be justified, a favorable cost-to-benefit ratio must be established based on recovery of capital costs through reductions in energy consumption. In order to assess accurately the impact of a given modification on the tunnel power requirements, a mathematical model of the tunnel is needed.

1.2 Objective

The objective of the present work has been to develop a mathematical model of Tunnel 16T which can be utilized to evaluate the net effect of potential tunnel modifications on the power requirements of the tunnel. The model consists of two computer programs hereafter referred to as the Historical Program and the Analytical Model. The Historical Program accesses tunnel data files for analysis of the tunnel performance as it exists and calculates pressure-loss coefficients for each of the tunnel components. The Analytical Model then utilizes these loss coefficients for the analysis of potential changes in tunnel component pressure losses with respect to the tunnel power. Both programs are designed for interactive graphics execution from a Tektronix® graphics terminal.

In Section 2.0, descriptions of the Tunnel 16T facility and components as well as the supporting systems are presented. In Section 3.0, the analytical approach is described and the controlling flow and thermodynamic equations are developed. In Section 4.0, the modeling procedure is outlined including the model options and functional flow diagrams. In Section 5.0, a description of the analysis of tunnel losses and the application of the math model for the evaluation of a potential tunnel modification is presented. In Section 6.0, conclusions and recommendations are given.

2.0 TEST FACILITY

2.1 General

The PWT 16-ft Propulsion Wind Tunnel (16T) is a closed-circuit, continuous-flow facility which can be operated over a Mach number range of 0.06 to 1.55. The stagnation pressure in this variable-density tunnel can be varied from 120 to 4,000 psfa (0.06 to 1.90 atm) depending on the Mach number. The tunnel stagnation temperature can be varied from a minimum of 60°F (289°K) to a maximum of 160°F (344°K) depending on the available cooling water temperature which varies with the time of year. The unit Reynolds number operational regime for Tunnel 16T is given in Figure 1 for an operating stagnation temperature of 110°F (80°F for $M < 0.6$). Additional information on the tunnel, its capabilities and operating characteristics are presented in Ref. 4.

2.2 Tunnel Components, Geometry, and Support Systems

The principal components and dimensions of the Tunnel 16T circuit are shown in Figure 2. The internal volume of the tunnel is 1.603×10^6 ft³. The major elements

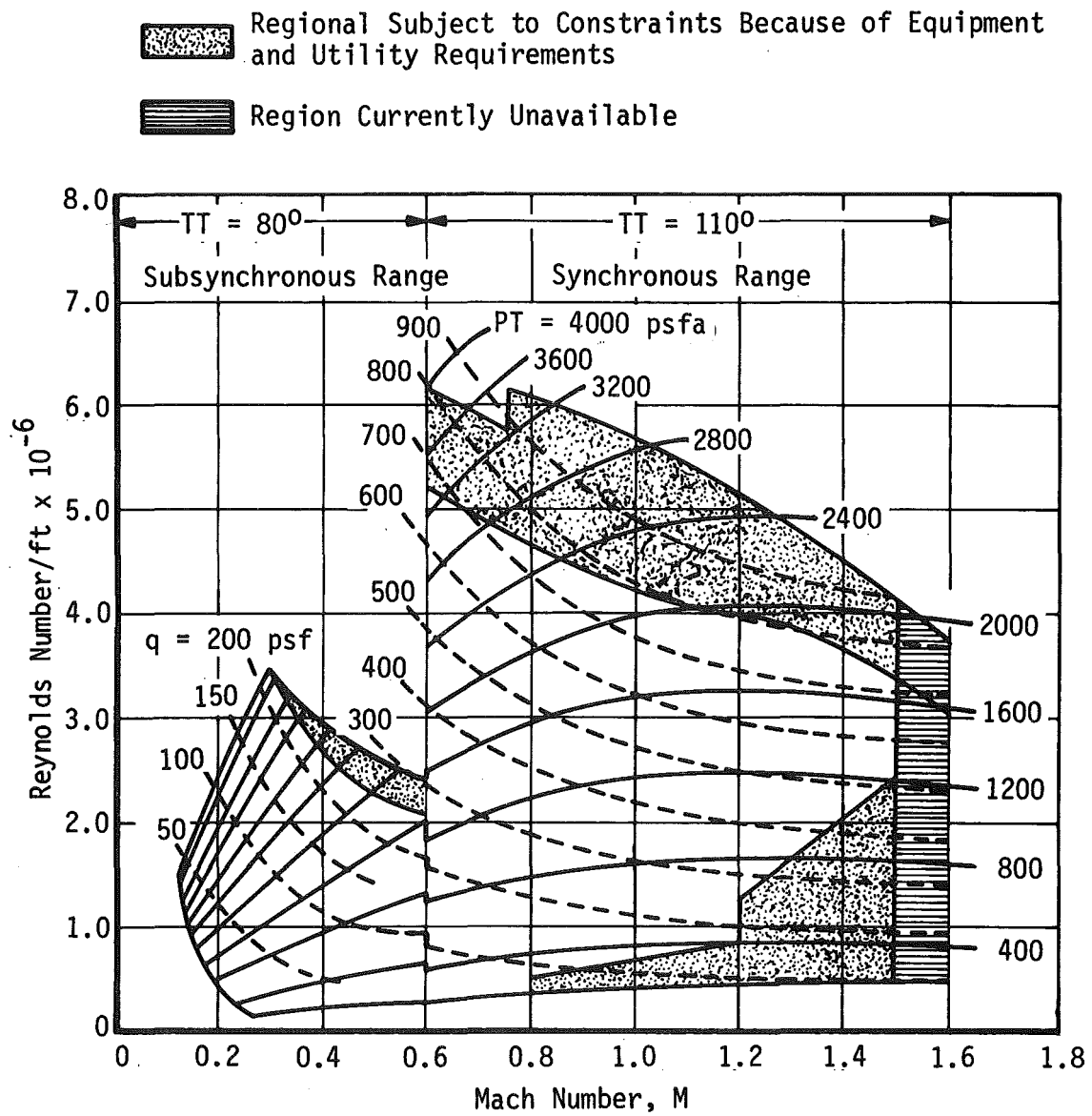
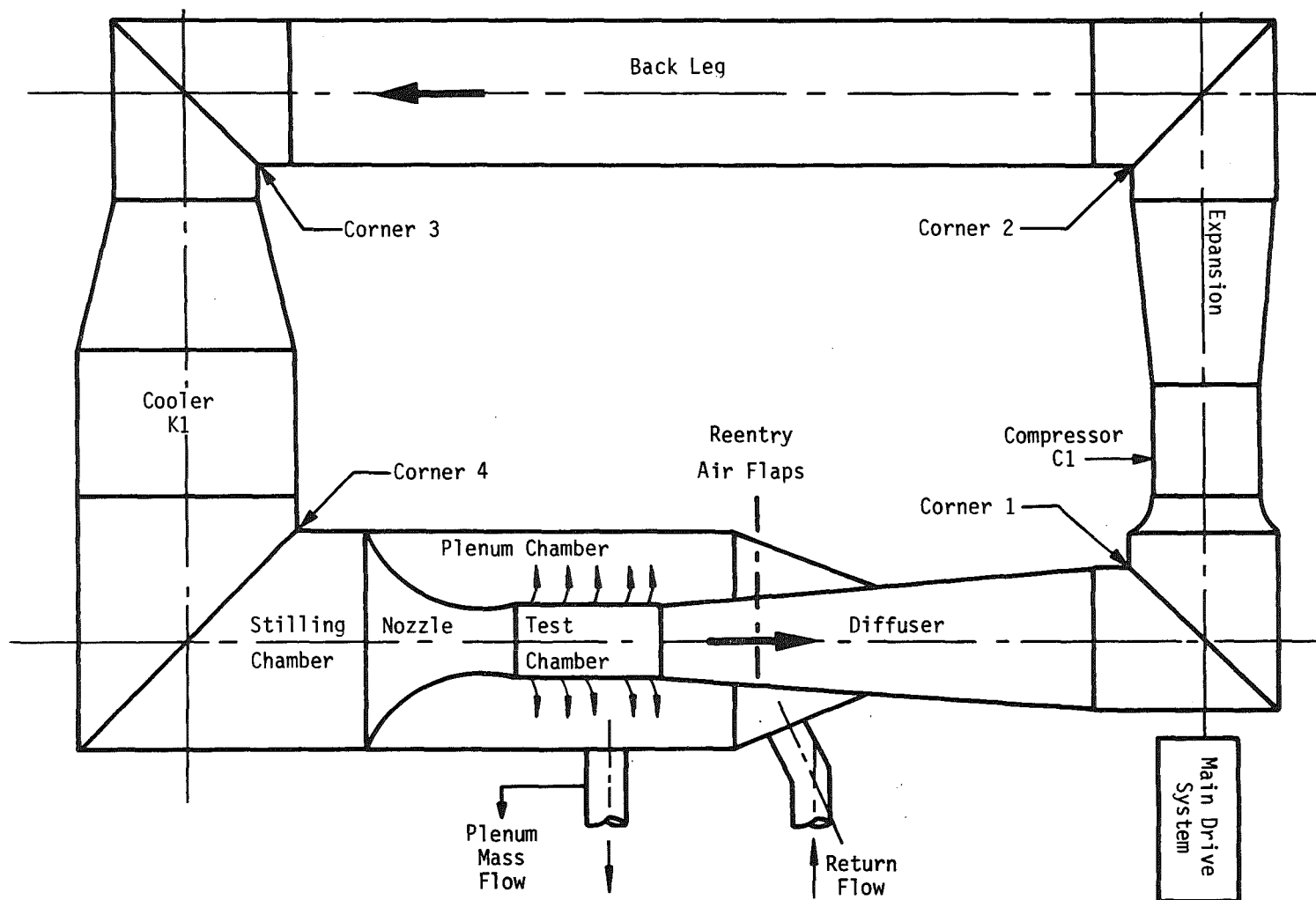
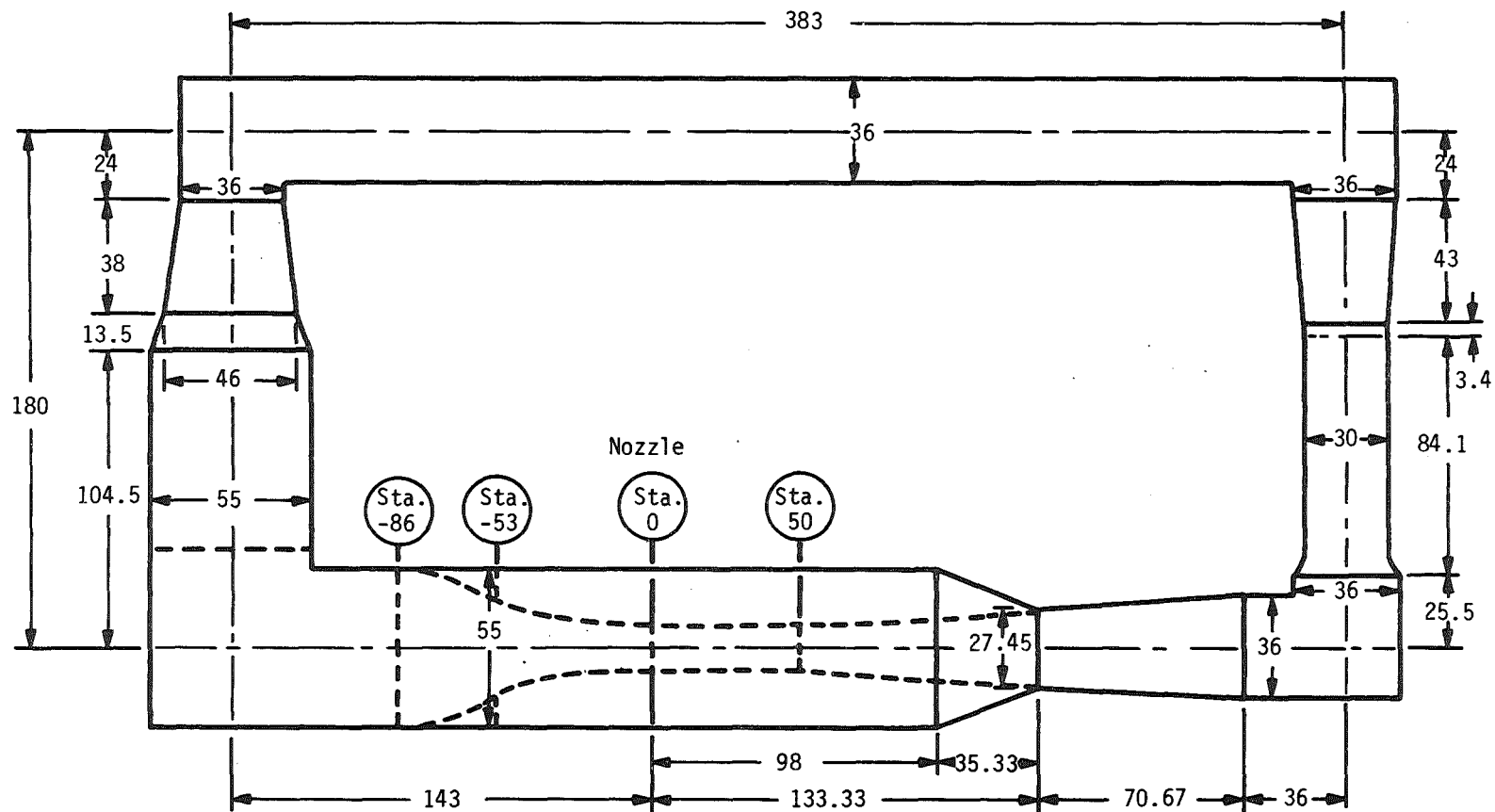


Figure 1. Operating Regime for Tunnel 16T.



(a) Major Components of Tunnel 16T

Figure 2. Components and Dimensions for Tunnel 16T.



Note: All Dimensions in Feet

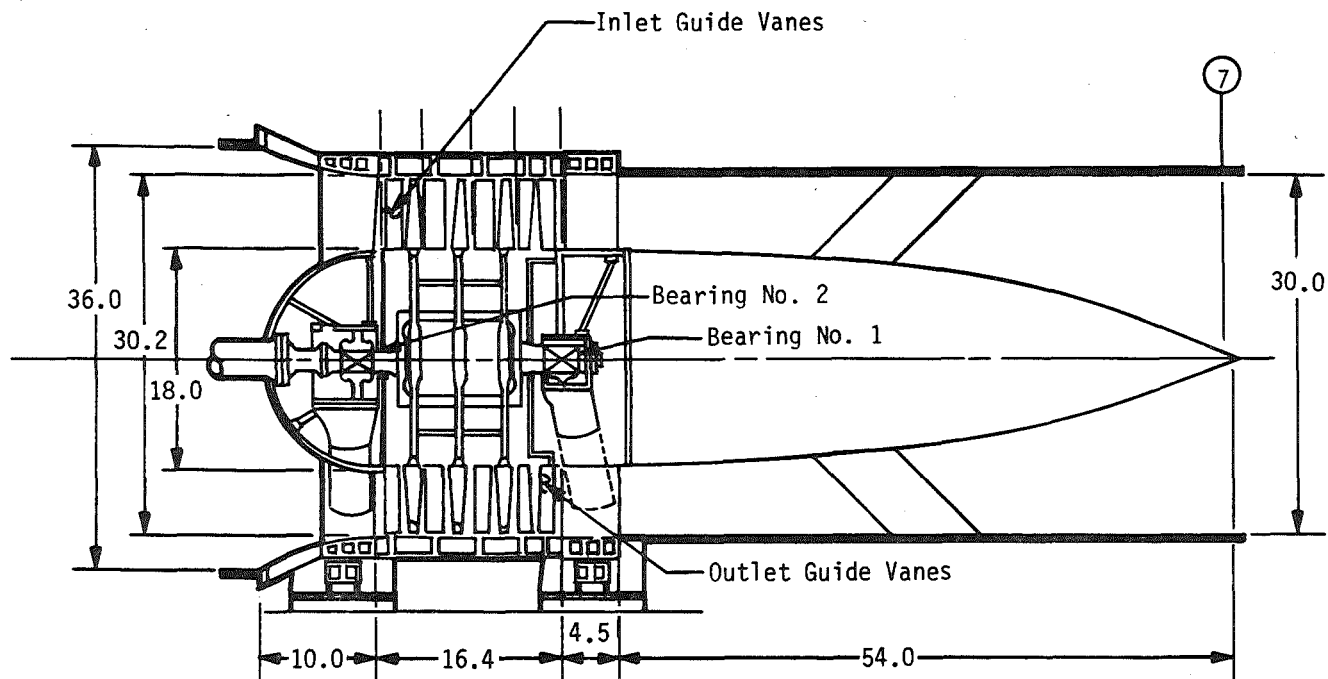
(b) Nominal Ducting Dimensions of Tunnel 16T
Figure 2. Continued.

and subsystems of this facility are identified and summarized below.

1. Main Drive System (MDS): The tunnel main drive system consists of four very large electric motors having a combined power rating of 236,000 hp. This includes two 83,000-hp synchronous motors and two 35,000-hp wound-rotor induction motors. The system can be operated up to 115 percent of the rated power or 292,300 hp. The induction motors function to bring the main drive system up to the synchronous speed of 600 rpm and for attaining Mach numbers less than 0.6 which requires subsynchronous variable-speed operation. Once at 600 rpm, the synchronous motors carry the majority of the load and operate at a higher efficiency than the induction motors.
2. Compressor (C1): The Tunnel 16T compressor is a three-stage, axial-flow machine. It is driven by the system of four

electric motor described above. The general arrangement of the compressor is shown in Figure 3. The design point of the compressor is an inlet volume flow of 200,000 cfs at a pressure ratio of 1.385 and an inlet temperature of 100°F. Aerodynamic design of the machine is based on the principle of a constant mean swirl. The blading consists of inlet guide vanes, interstage stator blades, rotor blades, and exit guide vanes. The inlet guide vanes, exit guide vanes, and rotor blades are cambered, twisted, and tapered. The inlet guide vanes and interstage stator blades are remotely controllable through the limits of +29 to -17 deg from the design point to allow specific selection of volume flows throughout the available range. The most recent performance map for the tunnel compressor is shown in Figure 4. A more detailed description of the C1 compressor may be found in Refs. 5 and 6.

3. Cooler (K1): The Tunnel 16T cooler is a finned tube, cross-flow air-to-water heat exchanger which has the purpose of removing the heat of compression of the main compressor from the



Design Conditions

Tip Speed, 942 ft/sec (Absolute)
 Hub Speed, 565 ft/sec (Absolute)
 Design Pressure Ratio, 1.385
 Design Inlet Volume Flow, 200,000 cfs
 Flow Coefficient, 0.47
 Work Coefficient, 0.308
 Inlet Axial Velocity, 442 ft/sec

Figure 3. Compressor C1 Layout for Tunnel 16T (Ref. 6).

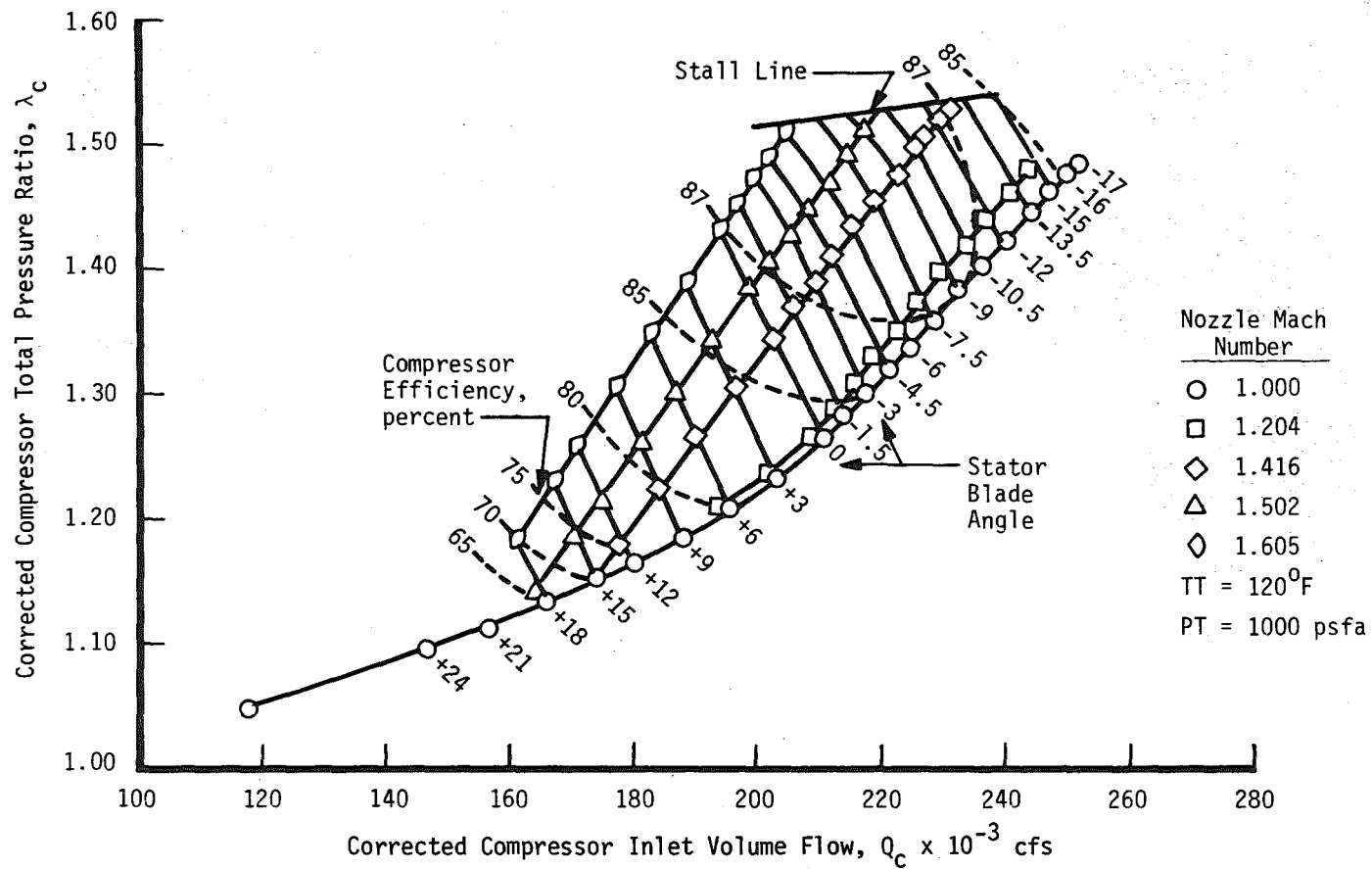


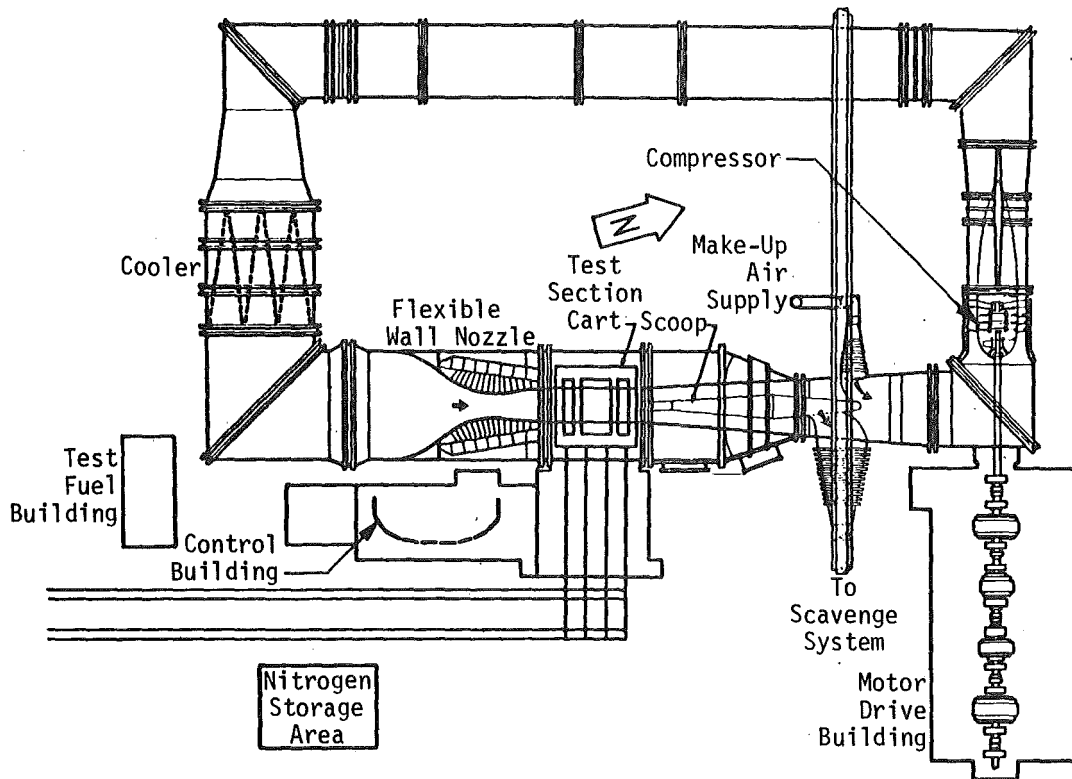
Figure 4. Compressor C1 Performance Map.

circuit. There are approximately 71 miles of 3/4-inch inside diameter, 1/8-inch wall, finned tubing in the cooler, with a total cooling surface area of 1.5×10^6 ft². The water flow rate to the cooler is controlled through a series of main and secondary control valves which provide the desired operating temperature within the available range. The water flow rate can be varied up to a maximum of 100,000 gpm. The available cooling water inlet temperature varies with the month of the year as shown in Table 1 (average values). For the operating range of Tunnel 16T, the minimum stagnation temperature will average about 20°F above the cooling water inlet temperature. The maximum allowable operating temperature is 160°F.

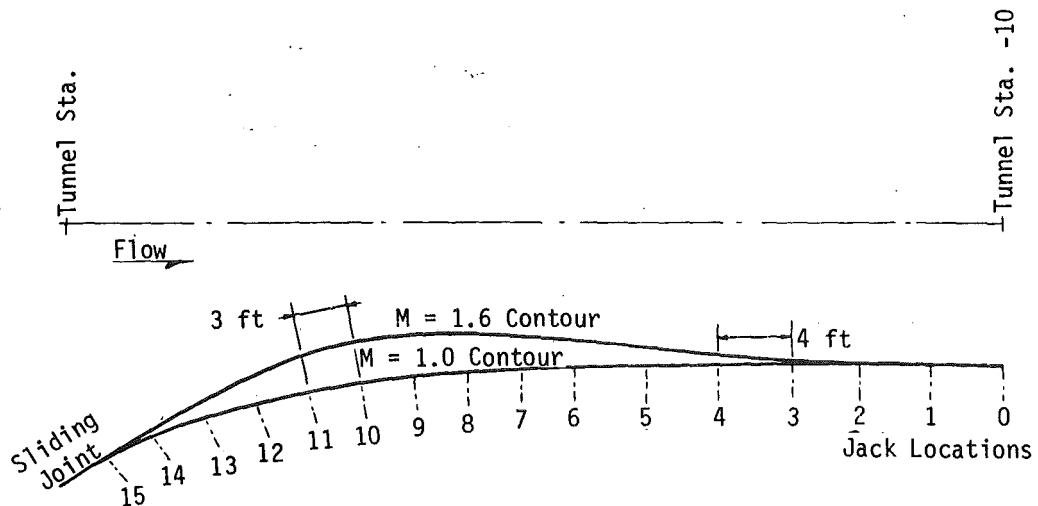
4. Flexible Nozzle: Supersonic Mach numbers in Tunnel 16T are obtained by using a flexible-wall, Laval-type nozzle. The contour of each sidewall is adjusted by 15 sets of electric-motor-driven jacks (or actuators). A schematic view of the flexible nozzle indicating the jack locations is shown in Figure 5. The nozzle contour can be adjusted from the

Table 1. Seasonal Cooling Water Temperatures (Ref. 4)

Month	Water Temperature OF	Month	Water Temperature OF
January	42	July	78
February	45	August	79
March	49	September	77
April	55	October	67
May	66	November	56
June	73	December	47



(a) Plan View Showing Nozzle Location



(b) Nozzle Contour Range and Jack Locations

Figure 5. Flexible Nozzle for Tunnel 16T.

sonic ($M=1$) contour to the $M=1.6$ contour in just over 11 minutes. In traversing this range the nozzle is set in 50 discrete steps in such manner as to avoid overstressing the steel nozzle plates. The nozzle is 54 ft in length, extending from a 16x32-ft entrance to a 16x16-ft exit.

5. Test Section: The test section is 16-ft square in cross section and 40-ft long. The entire test section and supporting structure are constructed as a separate integral unit which is removable from the tunnel. When installed in the tunnel the test section is enclosed by a plenum chamber which can be evacuated. The test section walls are perforated with 60-deg inclined-holes and have a porosity of 6 percent. To alleviate wall interference and unchoke the test section at supersonic Mach numbers, plenum suction is utilized to remove a portion of the test section flow through the porous walls. The test section sidewalls can be either converged or diverged 1 deg. Two test sections are available for use in Tunnel 16T. Test section 1 is used for propulsion and miscellaneous tests and can accommodate either

strut-, floor- or sidewall-mounted models. Test section 2 is used primarily for aerodynamic testing and is equipped with a sting support system.

6. Diffuser: The diffuser, shown schematically in Figure 6, is an annular-type diffuser with an effective 3.5-deg half-angle divergence. The diffuser consists of four major components: the rectangular section, the transition section, the conical section, and the scavenging scoop. The scavenging scoop is supported by two sets of vertical struts and a horizontal turnout strut. The compressor protective screen is presently mounted from the horizontal turnout strut. The diffuser is 160-ft long, approximately 16x16-ft square at the inlet, and has a 36-ft diameter at the exit.
7. Corners: The tunnel flow is routed through a 90-deg bend at four places in the rectangular-shaped Tunnel 16T circuit. At each corner, airfoil-shaped turning vanes are used to enhance the effectiveness of the flow-turning process. The corners are numbered 1 through 4 as shown in Figure 2. Corners 1, 2, and

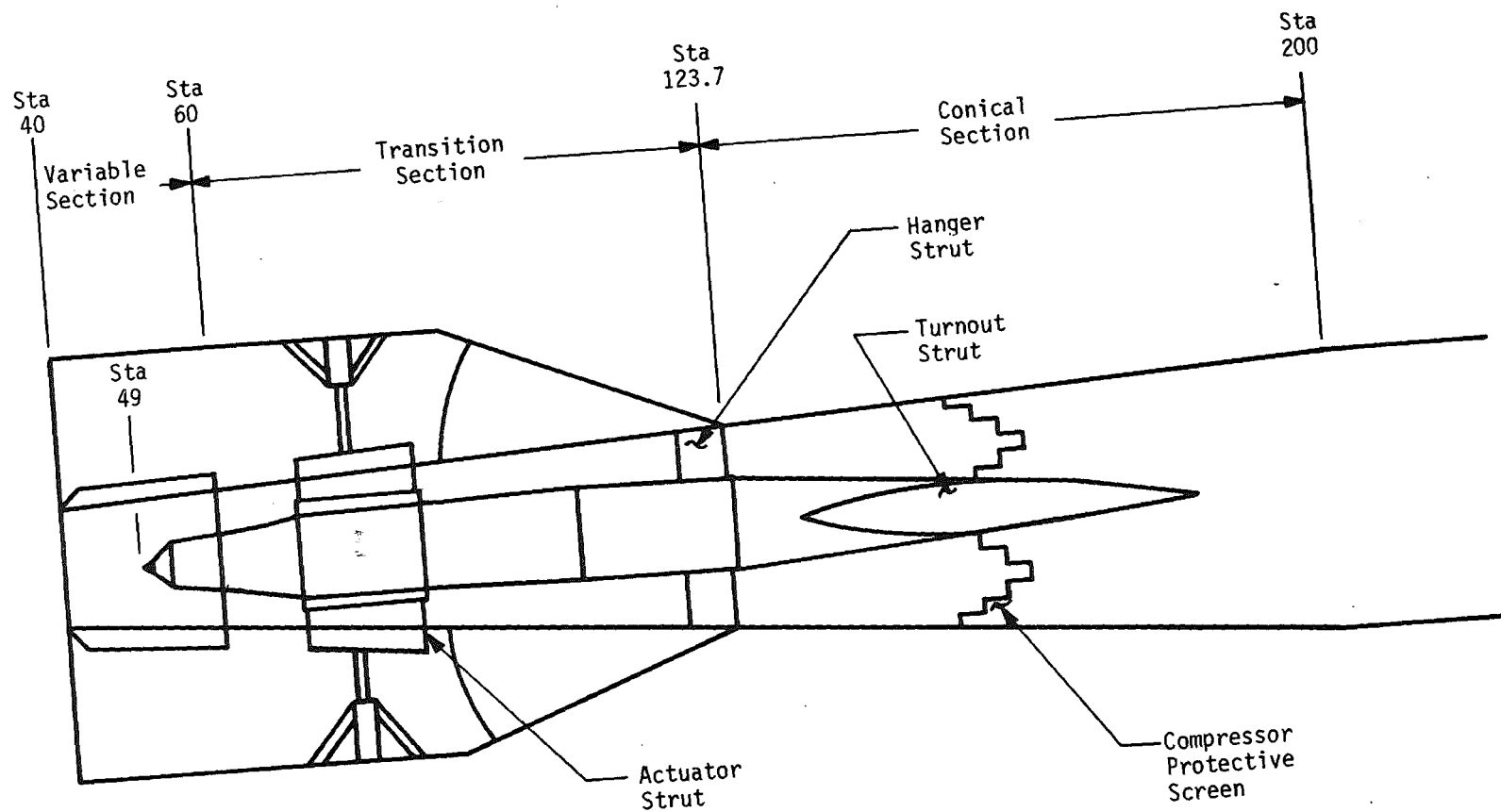


Figure 6. Diffuser for Tunnel 16T.

3 are 36-ft in diameter and corner 4 is 55-ft in diameter. In addition to the vanes, corner 1 has a 1x1-in. mesh, light-duty screen on the downstream end for compressor protection, and corner 4 has a wire mesh screen on the upstream end for particle contaminant control.

8. Atmospheric Drier: The PWT atmospheric drier provides dry air to the PWT wind tunnels to reduce the specific humidity of the tunnel air such that condensation does not affect the test data. The drier has two 570,000-lb dessicant beds to absorb moisture as ambient air is indrafted into the tunnel. Reactivation of the drier is accomplished using natural gas burners to drive out the moisture at about 400°F. The reactivation process typically takes from 12 to 14 hours to complete.

Summertime operation of the PWT wind tunnels presents the largest demand on the drier because of the inherently higher ambient dewpoints during this season.

9. Plenum Evacuation System (PES): The plenum evacuation system is a set of compressors which are used to support the operation of the PWT wind tunnels. The PES, which is shown in Figure 7, is divided into two sections (or increments) which can be operated either in parallel or independently. Each increment contains five 9-stage compressors which can be operated in parallel or staged in series for two-stage operations. Compressor units A, B, D, and E (see Figure 7) each contain two compressors and units C and F each contain one compressor. An additional seven-stage machine in each increment can be used for either two- or three-stage operations. The power rating of each increment is 77,500 hp; however, a continuous service factor of 15 percent allows an available power of 89,000 hp per increment. Two support functions for Tunnel 16T operation are performed by the PES which are referred to as suction flow and pressure control. Suction flow involves the removal of a portion of the tunnel main flow through the perforated test section walls, thereby unchoking the test section at near sonic speeds and reducing wall

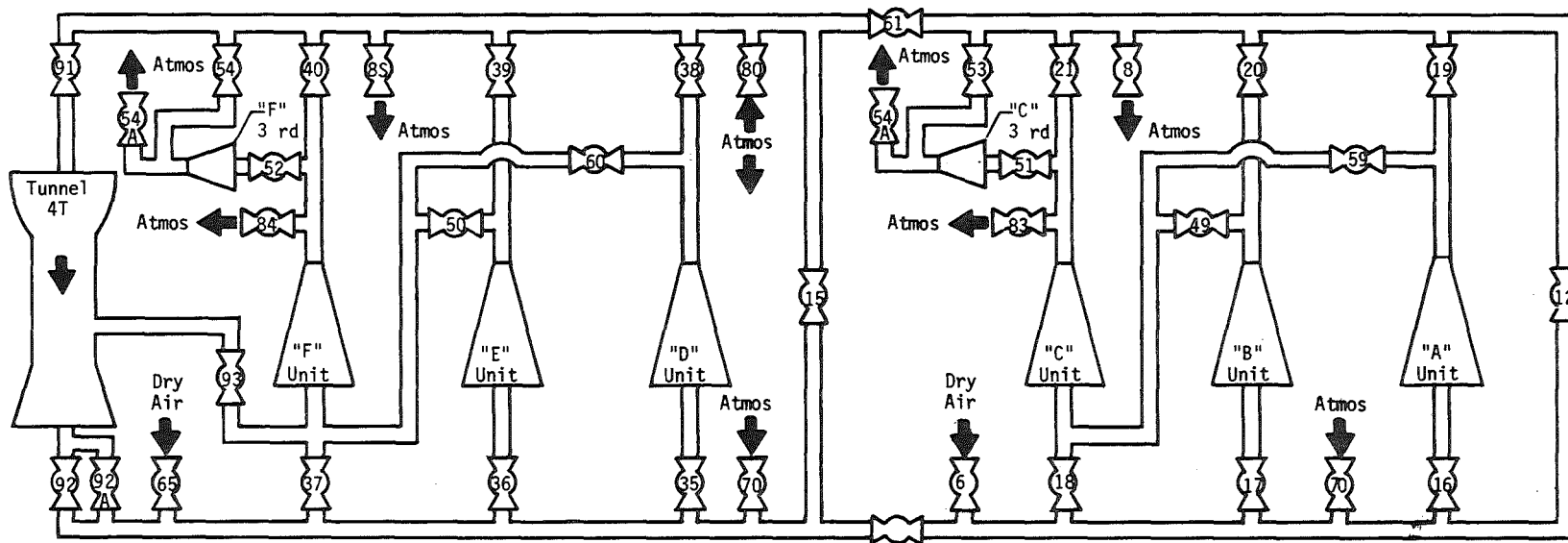


Figure 7. Schematic View of Plenum Evacuation System.

interference effects. This flow is returned to the tunnel through the reentry air flaps in the diffuser. Pressure control pertains to maintaining the test section stagnation pressure by either pumping air into the tunnel or exhausting tunnel air to atmosphere at stagnation pressures above or below atmospheric pressure, respectively. The pressure control function includes the introduction of dry makeup air into the tunnel to control the tunnel specific humidity.

Eg. 13

3.0 ANALYTICAL APPROACH

3.1 General

The historical approach to evaluating pressure losses in ducting systems such as wind tunnels is to divide the system into basic components and determine the pressure loss of each component. The pressure loss for components such as cylindrical sections, contractions, expansions, corners, screens, etc., are available from empirical compilations and empirically derived loss formulae. The total system pressure loss is equal to the summation of the various component pressure losses.

The approach used in developing the present model is similar to the aforementioned technique; however, a different methodology is utilized to assess the component pressure loss. Rather than dividing the facility into many discrete elements and calculating losses from frictional and profile drag using the aforementioned loss compilations and formulae, the facility is divided into a small number of components and the loss coefficients are measured. Tunnel performance is analyzed in the Historical Program which utilizes standard tunnel data to calculate the pressure loss of the tunnel components. In the Analytical Model the component pressure-loss coefficients

are either taken directly from the Historical Program results or are varied parametrically as program inputs. This approach reduces the number of tunnel ducting components to be analyzed and gives more accurate results for the total system.

3.2 Tunnel Component Model

For the model of Tunnel 16T, the facility was divided into the following eight components:

1. Main Drive System
2. Compressor C1
3. Cooler K1
4. Test Section
5. Diffuser
6. Corner 1
7. Backleg
8. Plenum Evacuation System

This division of tunnel components was chosen to be consistent with available tunnel instrumentation and to allow separation of functional components. The flow velocity and, hence, pressure loss of corners 2, 3, and 4, are small and they are, therefore, grouped together in the backleg component.

The model components are shown in a block diagram in Figure 8. All of the model components are divided by

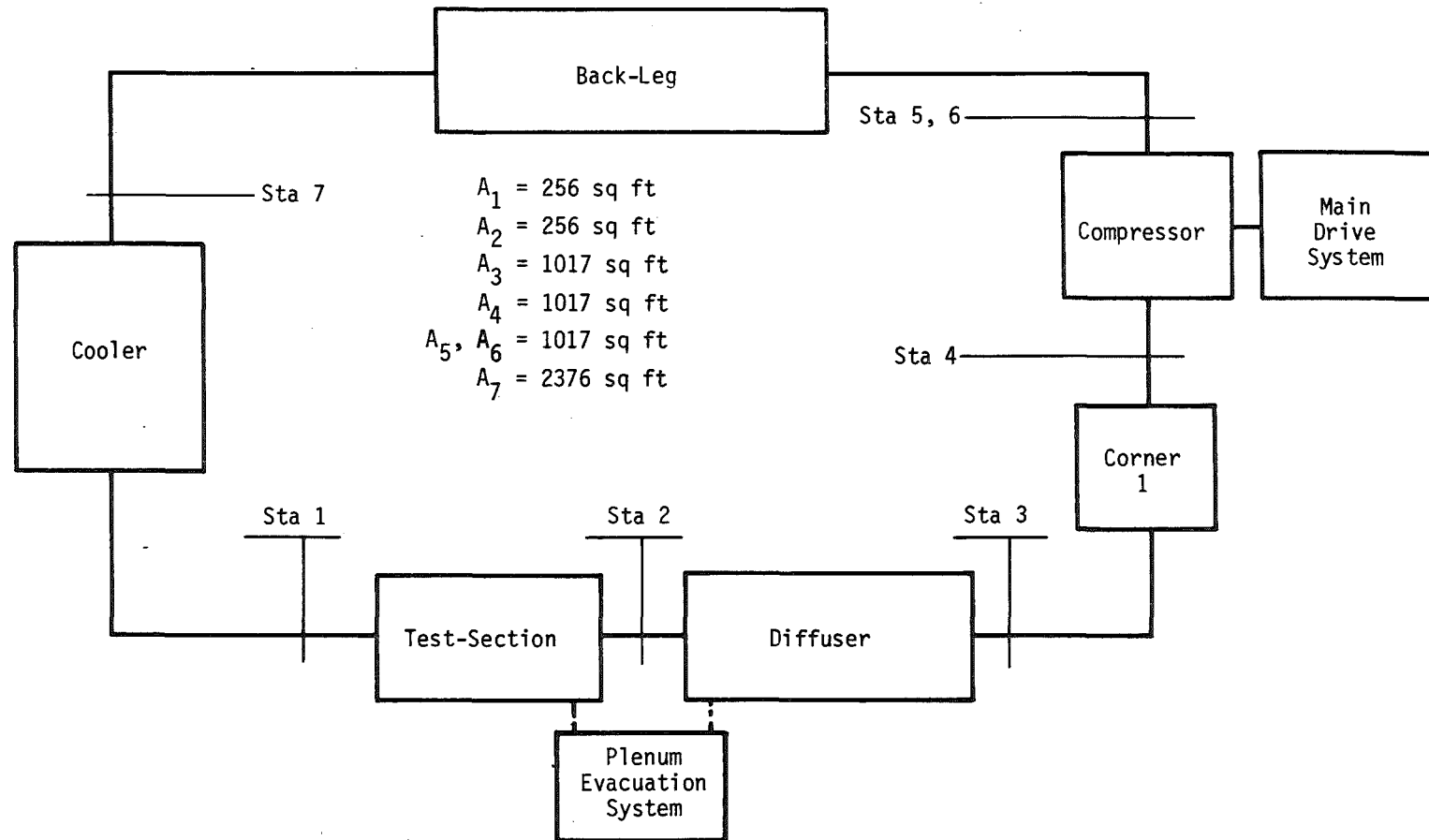


Figure 8. Component Model of Tunnel 16T.

function with the exception of the backleg which encompasses all of the tunnel components from the exit of the compressor C1 expansion to the inlet of the test section, and includes corners 2, 3, and 4, the cooler K1, the stilling chamber, and the nozzle. It is noted that, although cooler K1 is considered separately with regard to heat transfer, it is considered as an element of the backleg for pressure loss. Station numbers are assigned to the component functions as indicated in Figure 8. At the compressor exit, two station values, 5 and 6, are assigned; station 5 represents the state point for isentropic compression, and station 6 is the corresponding point for the actual polytropic compression.

3.3 Flow Equations

The principal concept involved in developing this model is the conservation of mass and energy within the ducting system. In addition, the following assumptions are made:

1. Tunnel walls are adiabatic
2. Steady flow
3. Perfect gas, air: $\gamma=1.4$;
 $R=53.35 \text{ ft-lbf/lbm-}^{\circ}\text{R}$
4. One-dimensional flow

The assumption of adiabatic tunnel walls has been previously investigated by M. H. Nesbitt of ARO, Inc. Analysis of results from his study indicates that the heat loss through the tunnel shell is directly proportional to the tunnel total temperature. The maximum heat loss through the shell at a tunnel total temperature of 580°R is around 5 percent. Tunnel 16T is very seldom operated at total temperatures above 580°R; therefore, the assumption is considered to be valid.

The flow computations start with specified conditions at the test section inlet (station 1). Calculation of flow conditions at the other tunnel stations is derived as follows.

The one-dimensional continuity equation for the tunnel flow process may be written as

$$W = \rho AV \quad (3-1)$$

The equation of state is

$$\rho = \frac{P}{RT} \quad (3-2)$$

and the speed of sound, c , is given by the relation

$$c = (\gamma RT)^{1/2} \quad (3-3)$$

which for air reduces to

$$c = 49.01(T)^{1/2} \quad (3-4)$$

The Mach number is defined as

$$M = \frac{V}{c} \quad (3-5)$$

and the isentropic relationship for static and total temperature in air is

$$T_T = T(1 + \frac{\gamma-1}{2} M^2) = T(1 + 0.2M^2)_{\text{air}} \quad (3-6)$$

Combining Eqs. (3-1) through (3-6) the mass flow can be expressed as

$$W = \frac{0.919}{(T_T)^{1/2}} PAM(1 + 0.2M^2)^{1/2} \quad (3-7)$$

Introducing the isentropic relationship for total and static pressure in air

$$P_T = P(1 + \frac{\gamma-1}{2} M^2)^{\frac{\gamma}{\gamma-1}} = P(1 + 0.2M^2)^{3.5}_{\text{air}} \quad (3-8)$$

Equation (3-7) may then be rewritten as

$$W = \frac{0.919}{(T_T)^{1/2}} (P_T)AM(1 + 0.2M^2)^{-3.0} \quad (3-9)$$

The mass flow at station 1, the test section inlet, is calculated using Eq. (3-9) for the specified test conditions. Assuming that the mass flow change resulting from pressure control is small, the mass flow is constant through each tunnel component except the diffuser. The mass flow through the diffuser is reduced by the flow removed through the porous walls of the test section. This flow is returned to the main flow in the middle of the diffuser, but in the model it is assumed to be returned at the exit. The flow through the diffuser is given by

$$W_2 = W_1 - WP \quad (3-10)$$

where the subscripts refer to tunnel station numbers, and WP is the plenum mass flow which is a measured quantity. The plenum mass flow is typically between 4 and 7 percent of the tunnel mass flow.

The static pressure at each tunnel station is measured using available static pressure orifices. In order to calculate the component pressure-loss coefficient, it is necessary to first calculate the Mach number and then total pressure at each station. These equations are derived as follows.

The stream impulse function is defined as

$$F = PA(1 + \gamma M^2) \quad (3-11)$$

Introduce the parameter \bar{F} such that

$$\bar{F} = \frac{F(\frac{\gamma}{R})^{1/2}}{W(TT)^{1/2}} = \frac{(1 + \gamma M^2)}{M(1 + \frac{\gamma-1}{2} M^2)^{1/2}} \quad (3-12)$$

Squaring this relation gives

$$\bar{F}^2 = \frac{\gamma^2 M^4 + 2\gamma M^2 + 1}{M^2(1 + \frac{\gamma-1}{2} M^2)} \quad (3-13)$$

which may be solved for M^2 using the quadratic equation to produce the following equation

$$M^2 = \frac{\bar{F}^2 - 2\gamma \pm [\bar{F}^4 - 2(\gamma+1)\bar{F}^2]^{1/2}}{(2\gamma^2 - (\gamma-1)\bar{F}^2)} \quad (3-14)$$

Eq. (3-14) reduces to

$$M^2 = \frac{-1 \pm [1 + 2(\gamma-1)\bar{W}^2]^{1/2}}{(\gamma-1)} \quad (3-15)$$

using the variable \bar{W} which is defined as

$$\bar{W} = \frac{W(TT)^{1/2}}{AP(\frac{\gamma}{R})^{1/2}} = M[1 + \frac{\gamma-1}{2} M^2]^{1/2} \quad (3-16)$$

It can be seen from Eq. (3-15) that only the positive root will produce a physical realistic (real number) solution. Therefore, Eq. (3-15) can be written as

$$M^2 = \frac{[(1 + 2(\gamma-1)\bar{W}^2)^{1/2} - 1]}{(\gamma-1)} \quad (3-17)$$

which for air is

$$M^2 = \frac{[(1 + 0.8 \bar{W}^2)^{1/2} - 1]}{0.40} \quad (3-18)$$

Solving Eq. (3-18) for M produces the necessary relation

$$M = 1.58113 [(1 + 0.8 \bar{W}^2)^{1/2} - 1]^{1/2} \quad (3-19)$$

which is used to calculate the Mach number at each tunnel station. The total pressure at each station may then be calculated using Eq. (3-8). The total pressure change across each component may then be calculated as

$$\Delta PT_{xy} = PT_x - PT_y \quad (3-20)$$

The pressure-loss coefficient for each component is expressed as

$$CPLR_{xy} = \frac{\Delta PT_{xy}}{q_x} \quad (3-21)$$

where the component inlet dynamic pressure is defined as

$$q_x = \frac{\gamma}{2} P_x M_x^2 = (0.7 P_x M_x^2)_{\text{air}} \quad (3-22)$$

Knowing the total pressure and Mach number at each station, one can calculate all of the flow parameters.

3.4 Compressor Relationships

The tunnel compressor system requires special consideration because, unlike any of the other circuit components, it is a pressure rise rather than a pressure-loss component. For steady-state tunnel conditions, the pressure rise across the compressor must be sufficient to overcome the pressure loss in the rest of the tunnel ducting components. The pressure rise across the compressor, ΔPT_{46} , is expressed as a function of the inlet total pressure, PT_4 , and compressor pressure ratio, λ , as

$$\Delta PT_{46} = PT_4 (\lambda - 1) \quad (3-23)$$

where the pressure ratio across the compressor is given by

$$\lambda = \frac{PT_6}{PT_4} \quad (3-24)$$

The flow rate through the compressor is expressed in terms of volume flow which is defined as

$$Q_4 = \frac{W_4 RT_4}{P_4} \quad (3-25)$$

In order to calculate the Tunnel 16T compressor performance in the Analytical Model for inlet temperatures other than the design (or calibration) temperature of 580°R, values of pressure ratio, λ , and inlet volume flow, Q , are corrected using the following fan-law relations, which are derived in Appendix A as

$$\lambda_c = \left[1 + \frac{TT_4}{580^{\circ}R} (\lambda^{1/3} - 1) \right]^{3.0} \quad (3-26)$$

$$Q_c = Q_4 \left(\frac{\lambda_c}{\lambda} \right)^{1/3} \quad (3-27)$$

In the Analytical Model, the corrected values of pressure ratio, λ_c , and volume flow, Q_c , are utilized to determine compressor efficiency, η_{comp} , using the data contained in Figure 4.

The total temperature rise across the compressor is calculated from the following equation for a polytropic compression, which is derived in Appendix B as

$$TT_6 - TT_4 = \frac{TT_4 (\lambda^{0.286} - 1)}{\eta_{\text{comp}}} \quad (3-28)$$

In order to calculate the power input to the Tunnel 16T compressor from the main drive system, the isentropic power imparted to the airstream by the compressor is first calculated by

$$HPI = CpW_4 TT_4 (\lambda^{0.286} - 1) \quad (3-29)$$

The compressor efficiency is defined as the ratio of isentropic shaft power, HPI, to the actual (polytropic) shaft power, HPP

$$\eta_{\text{comp}} = \frac{HPI}{HPP} = \frac{TT_5 - TT_4}{TT_6 - TT_4} \quad (3-30)$$

The shaft power input to the compressor is therefore given by

$$HPP = \frac{CpW_4 TT_4 (\lambda^{0.286} - 1)}{\eta_{\text{comp}}} \quad (3-31)$$

3.5 Main Drive System Model

The power input to the compressor C1 via the drive shaft from the main drive system is calculated for the polytropic compression knowing the compressor efficiency

in Eq. (3-31). The electrical power input to the main drive system, HPMDS, is equal to the compressor C1 shaft power, HPP, divided by the main drive system efficiency, η_{mds} . Thus,

$$\text{HPMDS} = \frac{\text{HPP}}{\eta_{\text{mds}}} \quad (3-32)$$

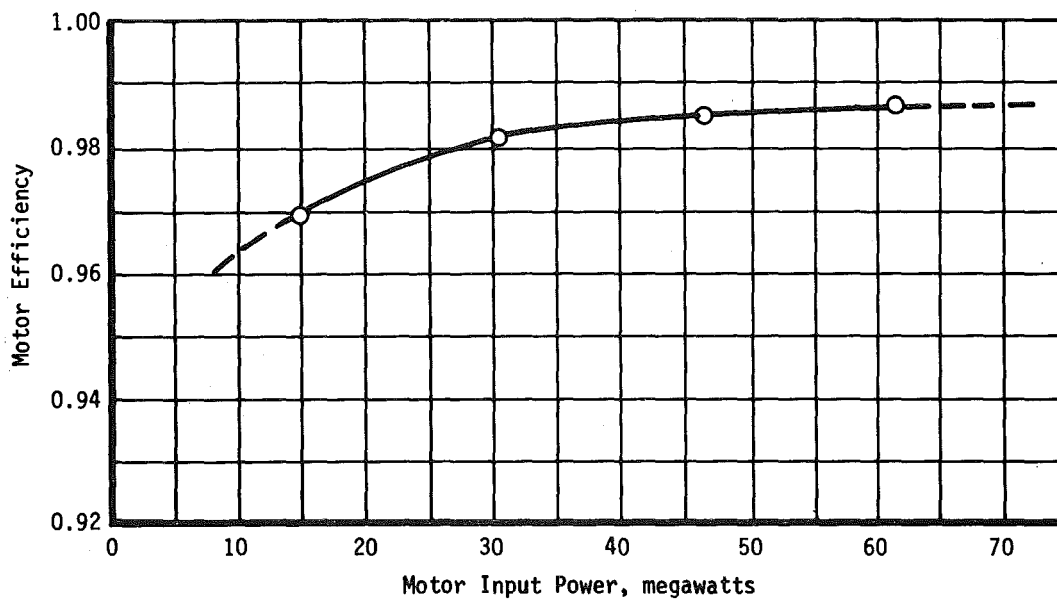
The PWT main drive system has four drive motors: two induction and two synchronous motors. Each type of motor has different efficiency characteristics which are shown versus input power in Figure 9. The total power input to the main drive system is equal to the sum of the four drive motor powers as

$$\text{HPMDS} = \text{HPM1} + \text{HPM2} + \text{HPM3} + \text{HPM4} \quad (3-33)$$

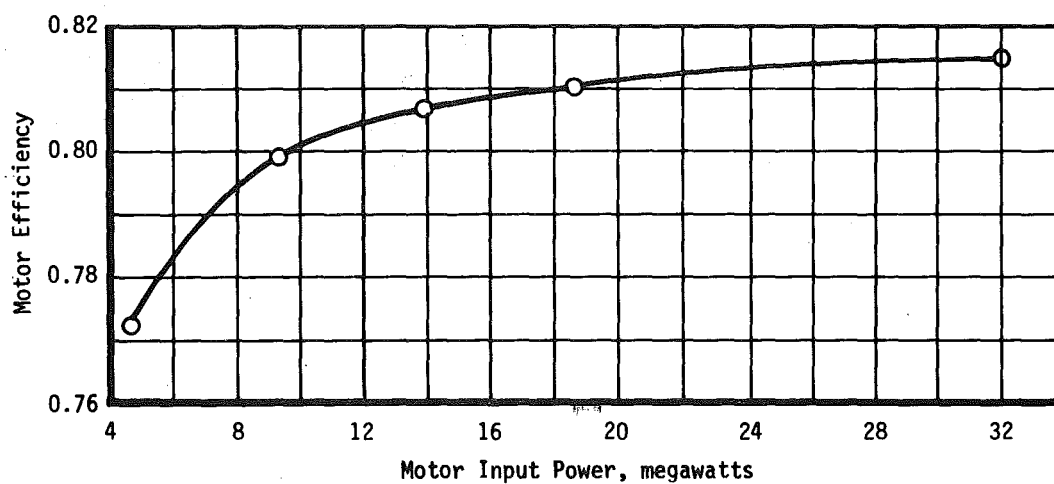
The efficiency of the main drive system is dependent upon the motor loading schedule and is given by

$$\eta_{\text{mds}} = \frac{\eta_{\text{M1}} \text{HPM1} + \eta_{\text{M2}} \text{HPM2} + \eta_{\text{M3}} \text{HPM3} + \eta_{\text{M4}} \text{HPM4}}{\text{HPMDS}} \quad (3-34)$$

In the Historical Program the power to the individual motor is known. The efficiencies in Figure 9 are used to calculate overall system efficiency, η_{mds} , and shaft power to the compressor.



(a) Synchronous Motor Efficiency



(b) Induction Motor Efficiency

Figure 9. Main Drive Motor Efficiencies.

In the Analytical Model the required compressor shaft power is assumed to be known and the power input to the main drive system must be calculated. To accomplish this a motor loading schedule based on operational experience is used. The loading schedule produces the relation for main drive system efficiency versus input electrical power shown in Figure 10. These data are contained in the program in the form of polynomial curvefits, one third-order equation for input power less than 137 MW, and a straight line (first-order) fit for values equal to and greater than 137 MW.

3.6 Thermodynamic Relationships

When operating at steady-state conditions, Tunnel 16T may be considered as an isolated thermodynamic system which receives work from an external source and exchanges heat with a single reservoir. The irreversibilities of the flow processes in the tunnel result in an increase in entropy. The input shaft work from the main drive system is degraded into thermal energy which is discharged through the tunnel cooler to the cooling water.

The total temperature-entropy diagram for the modeled flow process is shown in Figure 11. With the assumption of an adiabatic tunnel shell, entropy increases at constant total temperature from the inlet of

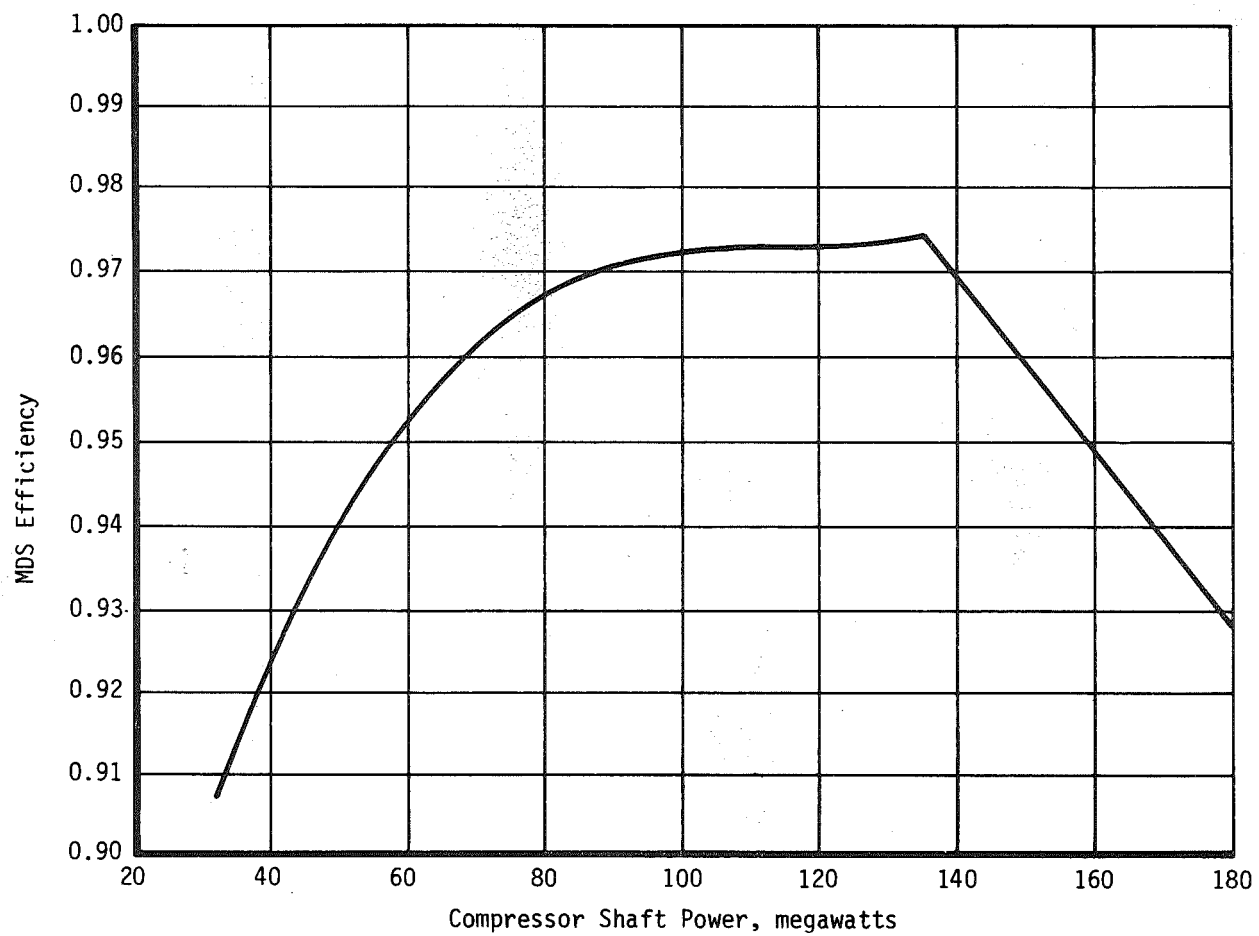


Figure 10. Main Drive System Efficiency.

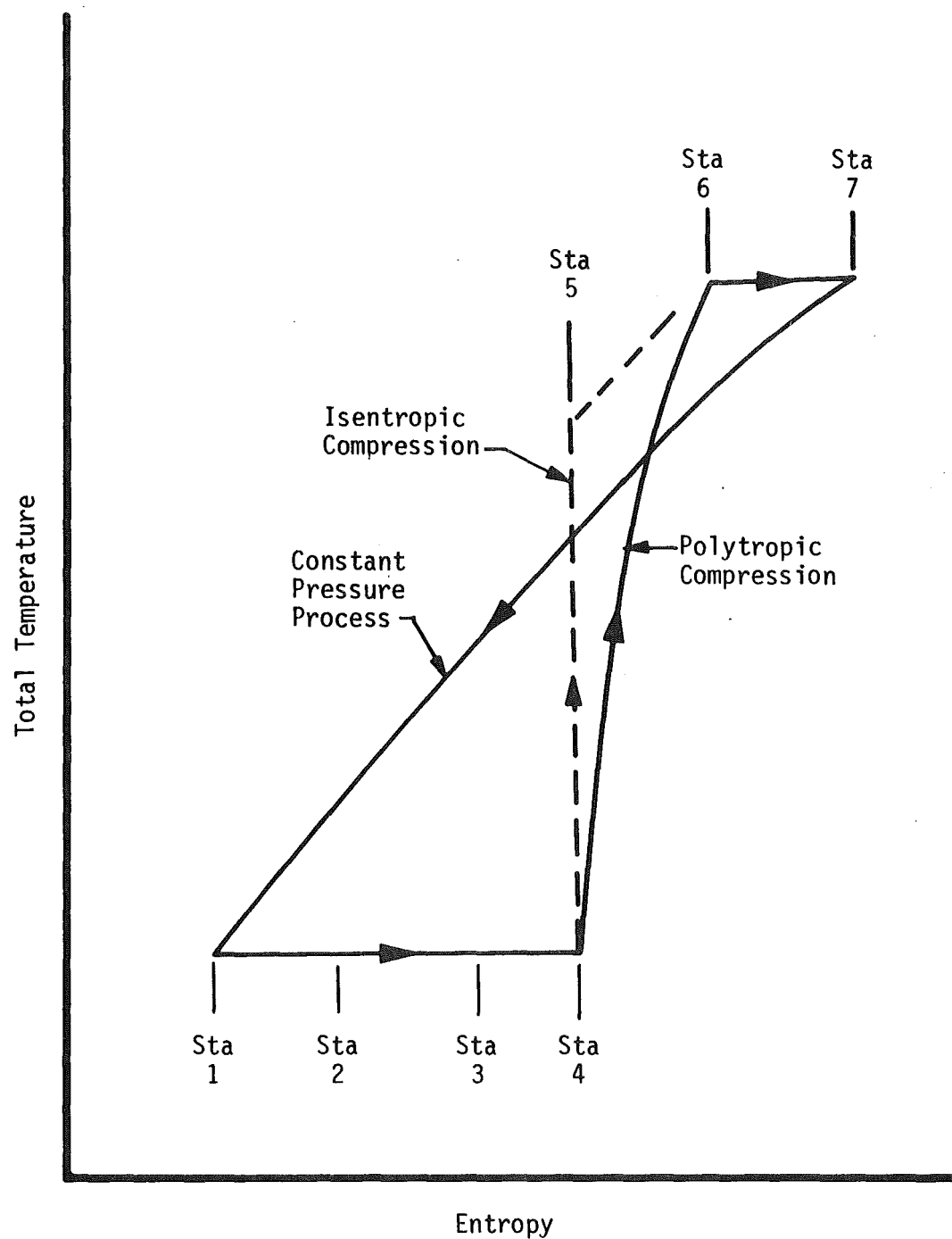


Figure 11. Total Temperature-Entropy Diagram for the Tunnel 16T Model.

the test section to the inlet of the compressor following the path 1-2-3-4. Through the compressor, an isentropic compression is indicated by path 4-5, while the actual polytropic compression is shown by path 4-6. Through the backleg, entropy again increases at constant total temperature, as shown by path 6-7. Then entropy decreases at constant pressure through the cooler indicated by path 7-1. (The cooler is considered separately from the backleg only in terms of temperature change.)

Analysis of entropy changes across tunnel model components is needed to assess the power dissipation for each component. The change in entropy across a tunnel component from temperature and pressure changes is given in Ref. 7 as

$$\Delta S_{xy} = -R \left[\ln \left(\frac{P_T^x}{P_T^y} \right) \right] + C_p \left[\ln \left(\frac{T_T^y}{T_T^x} \right) \right] \quad (3-35)$$

The availability of a steady flow system is defined as the maximum work that can be obtained from the system in a given state as it passes reversibly to the dead state, exchanging heat only with the surroundings. The dead state is the condition of a system when it is in thermodynamic equilibrium.

The change in availability across a tunnel component due to a change in entropy is then defined as

$$\Delta AVL_{xy} = T_{ds} (\Delta S_{xy}) \quad (3-36)$$

where T_{ds} is the dead-state temperature of the tunnel system.

Applying the First and Second Laws of Thermodynamics to the tunnel compressor and cooler, respectively, and noting that the work input to the compressor is equal to the heat removed through the cooler (again neglecting heat loss through the shell), gives

$$W_4 Cp(TT_6 - TT_4) = -W_7 T_{ds} \Delta S_{71} \quad (3-37)$$

By noting that the change in entropy from stations 7 to 1, ΔS_{71} , is related only to a temperature change, one can write the equation

$$\Delta S_{71} = Cp \left[\ln \left(\frac{TT_1}{TT_7} \right) \right] \quad (3-38)$$

Substituting Eq. (3-38) into (3-37) and noting that $W_4 = W_7$, one gets

$$TT_6 - TT_4 = T_{ds} \left[\ln \left(\frac{TT_7}{TT_1} \right) \right] \quad (3-39)$$

For the assumptions of total temperature change only across the compressor and cooler, it is known that $TT_7=TT_6$ and $TT_4=TT_1$. The dead-state temperature for the 16T tunnel model may now be written as

$$T_{ds} = \frac{(TT_6 - TT_1)}{\ln\left(\frac{TT_6}{TT_1}\right)} \quad (3-40)$$

Expanding the denominator in a Taylor series gives

$$\begin{aligned} \ln\left(\frac{TT_6}{TT_1}\right) &= 2\frac{(TT_6 - TT_1)}{(TT_6 + TT_1)} + \frac{2}{3}\left[\frac{(TT_6 - TT_1)}{(TT_6 + TT_1)}\right]^3 \\ &\quad + \frac{2}{5}\left[\frac{(TT_6 - TT_1)}{(TT_6 + TT_1)}\right]^5 + \dots \quad (3-41) \end{aligned}$$

The quantity $(TT_6 - TT_1)$ is the total temperature change across the cooler which is typically in the range of 40 to 100°R. The quantity $(TT_6 + TT_1)$ is on the order of 1,200°R. Substitution of these values into Eq. (3-41) shows that the cubic term is less than 0.5 percent of the first-order term. Therefore, in the range of total temperature operation in Tunnel 16T, Eq. (3-41) may be approximated by

$$\ln\left(\frac{TT_6}{TT_1}\right) = 2\frac{(TT_6 - TT_1)}{(TT_6 + TT_1)} \quad (3-42)$$

Eq. (3-40) may now be written as

$$T_{ds} = \frac{(TT_6 + TT_1)}{2} \quad (3-43)$$

which is used to calculate the dead-state temperature for each set of test conditions.

For the tunnel pressure-loss components, the inlet and exit total temperatures are equal; therefore, the decrease in availability is due only to the change in total pressure

$$\Delta AVL_{xy} = T_{ds} \left[-R \left(\ln \left(\frac{PT_x}{PT_y} \right) \right) \right] \quad (3-44)$$

The dissipation of power across a tunnel component because of the change in availability is given in Ref. 7 as

$$PD_{xy} = W_x (\Delta AVL_{xy}) \quad (3-45)$$

The total-power dissipation of Tunnel 16T is calculated as the sum of the individual component power dissipation values by

$$PDWT = PD_{12} + PD_{23} + PD_{34} + PD_{46} + PD_{67} \quad (3-46)$$

In order to evaluate the relative magnitude of the power dissipation of each component with respect to the

total power dissipation of the wind tunnel, the fractional power dissipation is calculated as a percentage of the total as

$$FDP_{xy} = \frac{PD_{xy}}{PDWT} \quad (3-47)$$

The power extracted from the airstream as heat by transfer to the cooling water is calculated by

$$H = W_7 C_p (TT_7 - TT_1) \quad (3-48)$$

This completes the thermodynamic analysis equations. The remaining analysis of the primary tunnel support system, the PES, will be discussed in the next section.

3.7 Plenum Evacuation System Model

An empirical model of the Plenum Evacuation System (PES) is utilized in the Analytical Model to calculate the power and compressor configurations of this system. As described in Section 2.0, the PES is a set of compressors divided into two sections or increments which are used to support the operation of the PWT wind tunnels.

For Tunnel 16T, this support primarily involves two distinct functions hereafter referred to as suction flow and pressure control.

Suction flow involves the removal of a portion of the test-leg flow through the plenum and is normally utilized for test section Mach numbers greater than 0.75. The ratio of the pressure at the diffuser reentry flaps to the pressure in the plenum chamber (Figure 2) is small and, therefore, only one stage of compressors is required for suction flow. However, the volume flow is large and as many as nine compressors in parallel may be required depending on the model blockage. (Model blockage is defined as the maximum model cross-sectional area divided by the test section area.) The number of compressors required for suction flow is determined by the suction volume flow requirements.

A PES compressor performance map, Figure 12, shows that the compressor volume flow is nearly constant in the lower pressure ratio range for a given inlet-guide-vane setting. In the PES algorithm, each compressor is assumed to have a constant nominal volume flow of 4,500 cfs. This conservative estimate was selected to allow for ducting losses in the PES. The total suction volume required for a given condition is divided by 4,500 and rounded up to the next highest whole number to obtain the

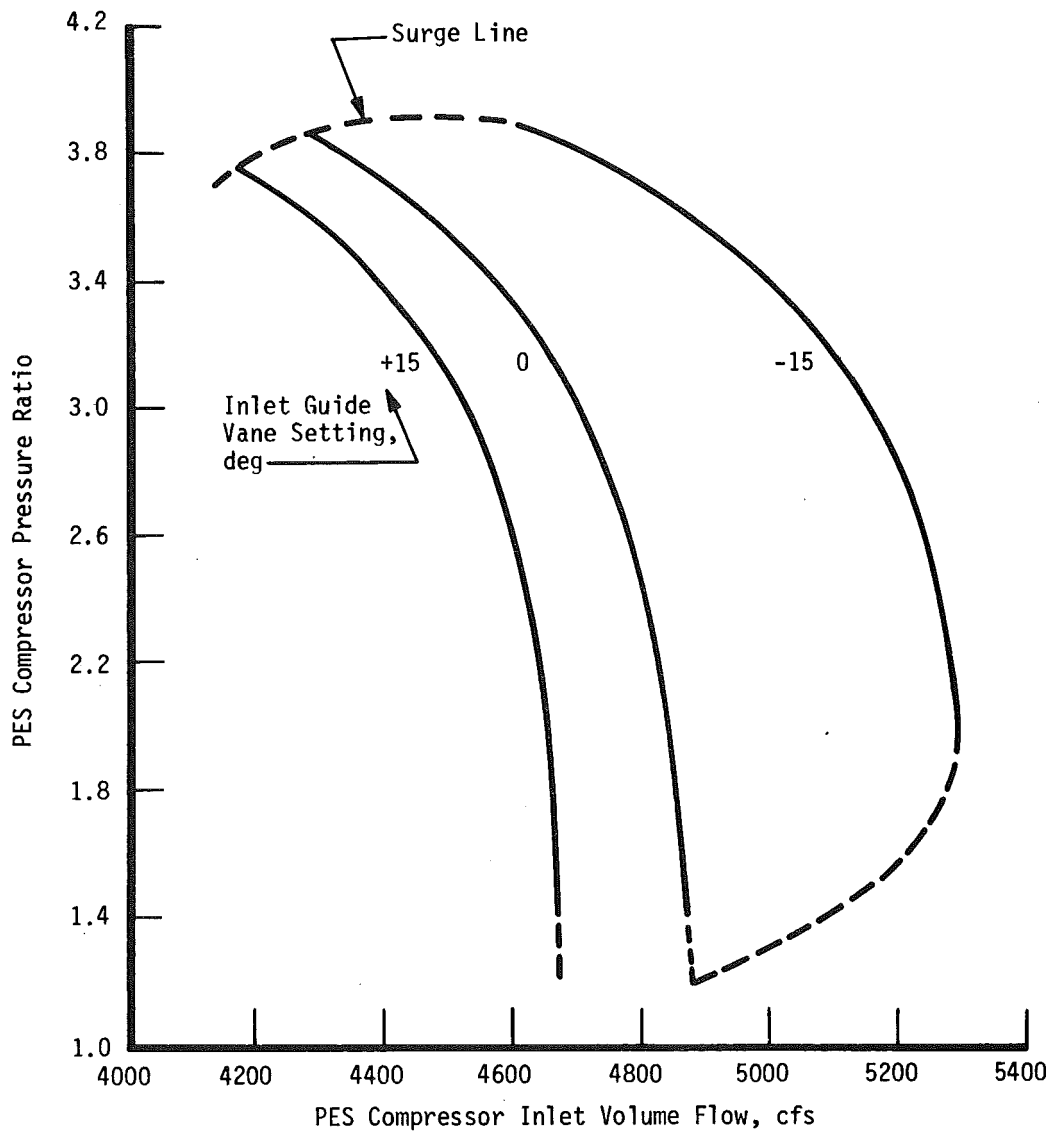


Figure 12. Performance Characteristics of Plenum Evacuation System First- and Second-Stage Compressors for an Inlet Temperature of 100°F.

number of suction flow compressors required. Two PES increments are required when the number of compressors exceeds five.

For pressure control, as many as three stages of compressors may be necessary to maintain very low tunnel pressures. The number of pressure control stages required is defined in Table 2. The volume flow requirements of the pressure control machines are relatively small (compared to the suction flow), so fewer compressors per stage are required. The number of compressors required for pressure control is assigned based on the number of stages and the test section Mach number as shown in Table 3. This scheme of compressor assignment is considered conservative in that the designated configurations can always maintain the required volume flows. The pressure control stage requirements are shown superimposed on a Tunnel 16T operating envelope in Figure 13. The division of the three-stage operation into an additional PES configuration for $M \geq 1.0$ is necessary because of tunnel drying difficulties which are normally encountered in that portion of the operating range. Pressure control always requires only one increment of the PES and is arbitrarily assigned to the second increment.

Table 2. PES Pressure Control Staging Regimes

Test Section Static Pressure	Number of Stages
$P > 700$ psfa	1
$250 < P \leq 700$ psfa	2
$P \leq 250$ psfa	3

Table 3. PES Pressure Control Compressor Configurations

Stages	Mach No.	Compressors	Configuration
1	All	1	1 in stage 1
2	All	3	2 in stage 1 1 in stage 2
3	$M < 1.0$	4	2 in stage 1 1 in stage 2 1 in stage 3
3	$M \geq 1.0$	6	4 in stage 1 1 in stage 2 1 in stage 3

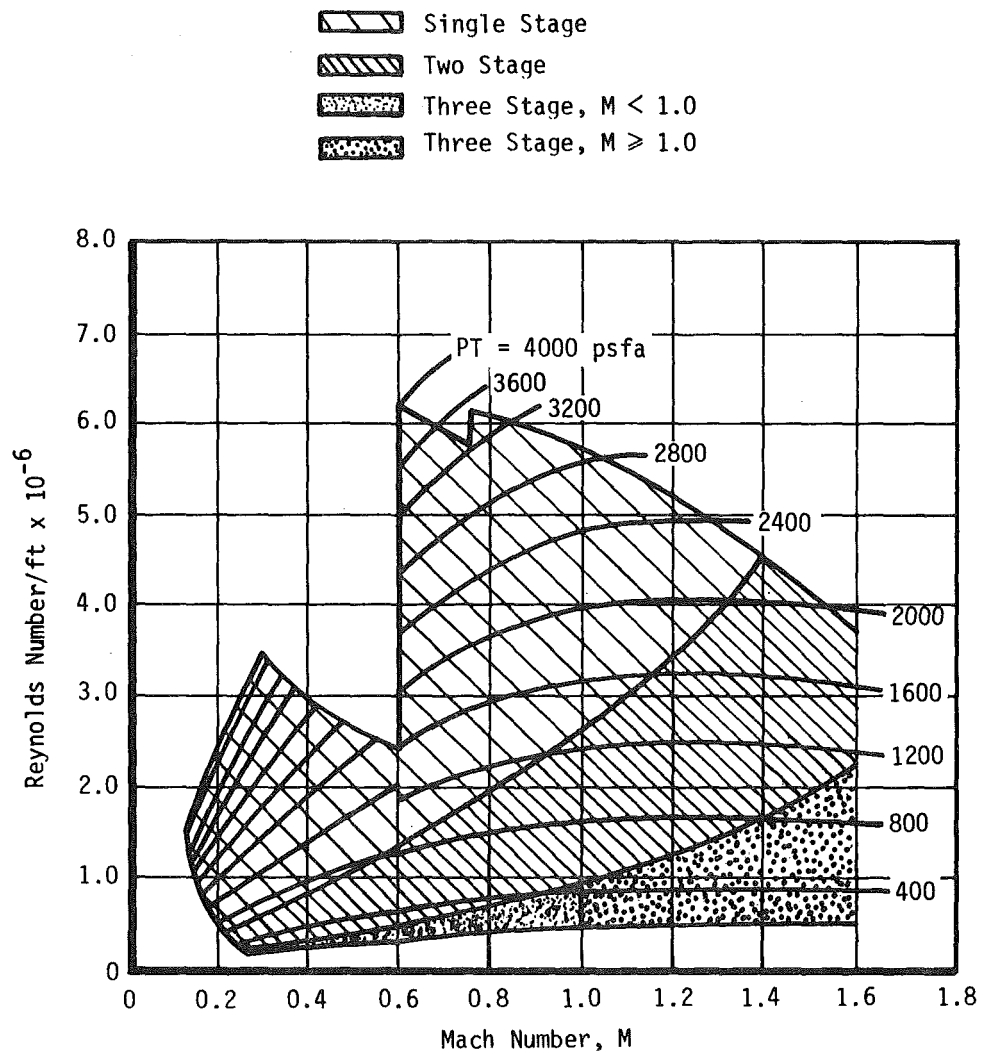


Figure 13. PES Pressure Control Staging Regimes in Tunnel 16T.

The PES compressor configuration is identified by the use of a code which is given in the following format:

$$\text{CONPES} = \text{X.XX} \quad (3-49)$$

The digit to the left of the decimal point is the increment identification (1, 2, or 3 for both increments). The first digit to the right of the decimal point identifies the number of stages, and the second digit to the right of the decimal point is the number of compressors in the first stage. The algorithm computes a separate PES configuration for each support function.

The pressure ratios across the PES compressors are needed for computing the power requirements for each compressor and the PES as a whole. For suction flow, the pressure ratio is the same for each compressor and is assumed to be equal to the static pressure at the inlet to the compressor divided by the test section static pressure. The PES ducting losses between the tunnel and the inlet and exhaust headers of the PES are assumed to be negligible. The assumptions have been verified by previous plant system experimentation. For pressure control, the overall PES pressure ratio formula used depends upon whether the tunnel stagnation pressure is above or below atmospheric pressure. For tunnel stagnation pressures below atmospheric pressure, the PES pressure control

pressure ratio is equal to atmospheric pressure divided by the test section free-stream static pressure. For tunnel stagnation pressures above atmospheric pressure, the PES pressure control pressure ratio is equal to the PES suction flow pressure ratio. For multiple staging configurations, the stage pressure ratios are defined in Table 4.

The power requirements to drive the PES compressors are computed from accumulated operational data in the form of a polynomial curvefit equation. For compressors of the first and second stages, the power can be expressed as a function of the discharge pressure, DP, and the machine pressure ratio, PR, using the polynomial equation

$$MWC = \frac{DP}{-233.1 + 445.3(PR) - 135.6(PR)^2 + 14.6(PR)^3} \quad (3-50)$$

The stage power requirement is equal to the product of the PES compressor drive power and the number of compressors in the stage.

The third stage compressor in each increment is smaller in size than the first and second stage machines. Consistent with operational data, the drive power for the third stage compressor is 2 MW.

Table 4. PES Compressor Pressure Ratios
for Multiple Stage Configurations

Stages	Pressure Ratios
1	$PRS1 = PRPES$
2	$PRS1 = 3.0$
	$PRS2 = \frac{PRPES}{3.0}$
3	$PRS1 = \frac{PRPES}{5.4}$
	$PRS2 = 3.0$
	$PRS3 = 1.8$

The total plenum evacuation system power is then obtained as the sum of the individual pressure control stage powers and the suction flow power as

$$MWPES = MWS1 + MWS2 + MWS3 + MWSF \quad (3-51)$$

4.0 MODELING PROCEDURE

4.1 Historical Program

The calculation procedure for the Tunnel 16T Historical Program is shown in the flow chart of Figure 14. With known test section inlet conditions, station 1, and measured static pressures at stations 2, 3, and 4, the tunnel mass flow and the flow conditions at stations 2, 3, and 4 are calculated using Eqs. (3-9), (3-19), and (3-8), respectively.

Solution for conditions across the compressor cannot be solved explicitly; therefore, iteration is required. The compressor pressure ratio, λ , which is measured, is based on static pressures; however, the total pressure ratio is required for calculation of both the exit total temperature, TT_6 , and the compressor efficiency, η_{comp} . Iteration is initiated by equating the compressor total pressure ratio to the measured static pressure ratio. Equation (3-24) gives an initial value for the total pressure at the compressor exit, PT_6 . The compressor efficiency is then calculated from Eq. (3-30) and the actual compressor shaft power, HPP , is solved from Eq. (3-32). Next, an initial value of the compressor exit total temperature, TT_6 , is calculated from Eq. (3-28).

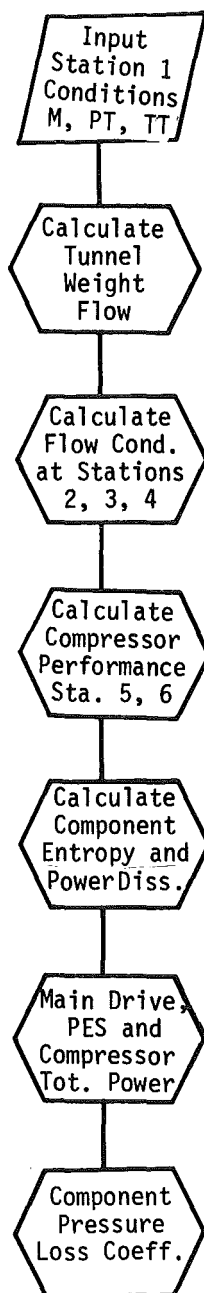


Figure 14. Historical Program Flow Chart.

Using this value of TT_6 , a Mach number at the compressor exit, M_6 , is calculated from Eq. (3-19). Mach number M_6 is used to correct the compressor exit total pressure, PT_6 , from Eq. (3-8), and the process is repeated. The iteration is terminated when a tolerance of $0.01^\circ R$ between successive values of TT_6 is achieved.

The entropy change and power dissipation across each of the tunnel components is calculated from Eqs. (3-35) and (3-45), along with the fractional power dissipation in percent of total main drive power from Eq. (3-47).

The pressure-loss coefficient for each of the tunnel components is calculated using the total pressure differentials, ΔPT_{xy} , and component inlet dynamic pressure, q_x , using Eq. (3-21). The pressure-loss coefficients for each of the tunnel components are plotted versus the test section Mach number and a polynomial curvefit is applied to each. The polynomial equation is

$$CPLR_{xy} = \sum_{i=0}^5 K_i M_1^i \quad (4-1)$$

where K_i ($i=0$ to 5) are the polynomial coefficients.

The coefficients of the curvefits are tabulated for input to the Analytical Model. A sample set of tunnel component curvefits with the polynomial coefficients is shown in Figure 15.

In addition to determination of the loss coefficients for use in the Analytical Model, the Historical Program may be used for analysis of tunnel performance using an XY or diagrammatic plot option. A sample of each is shown in Figure 16. The XY plot format can be utilized for displaying any two tunnel parameters. The diagrammatic plot displays the distribution of power dissipation for a selected data point.

4.2 Analytical Model

The calculation procedure for the Tunnel 16T Analytical Model is shown in the flow chart in Figure 17. Test section Mach number, total pressure, and total temperature are program inputs which define the conditions at station 1. The stored polynomial pressure-loss coefficients provide the necessary information, using the polynomial equation, Eq. (3-52), to solve for the flow conditions at stations 2, 3, and 4. An iteration similar to the one used in the Historical Program provides conditions across the compressor utilizing a table-look-up

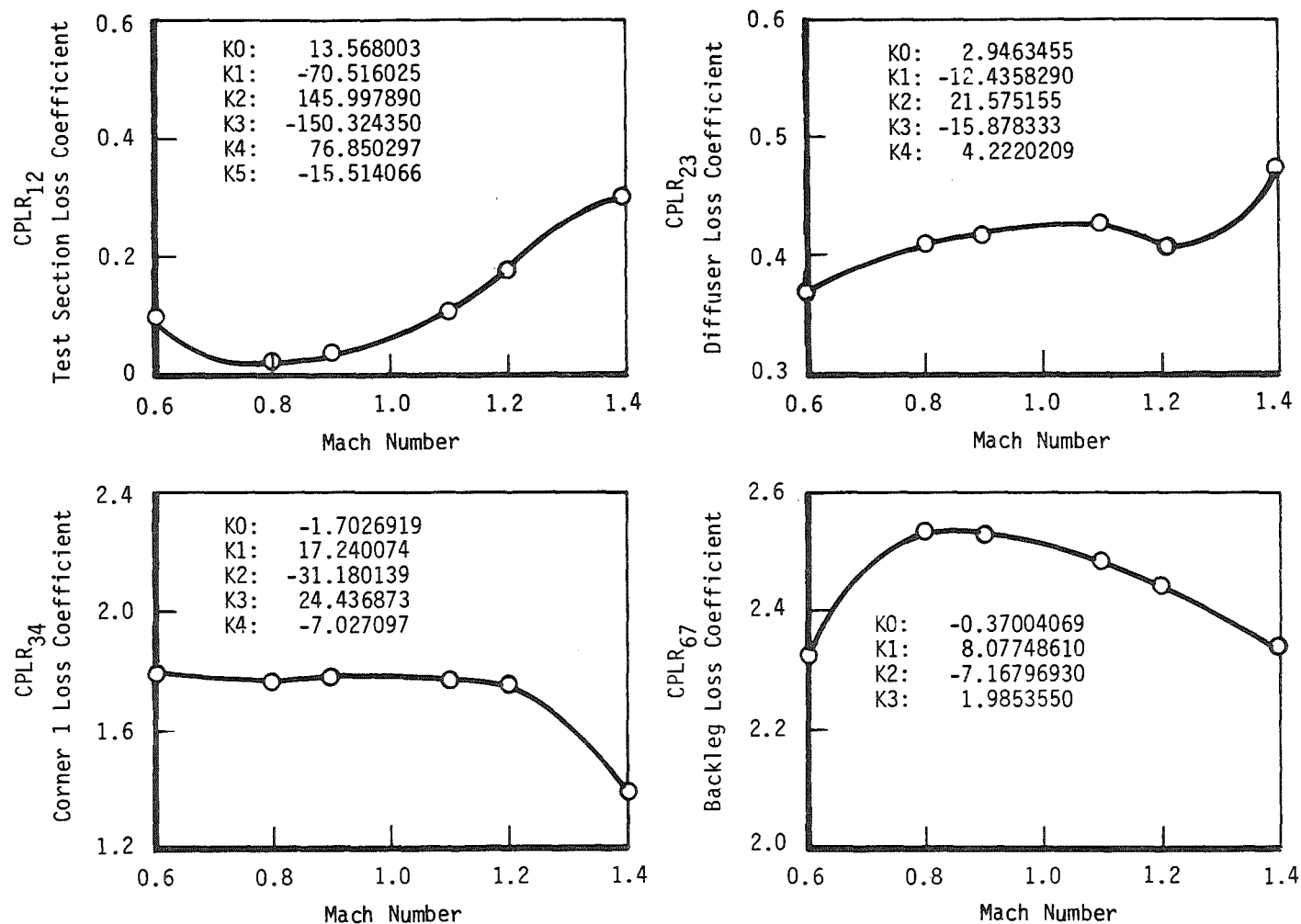
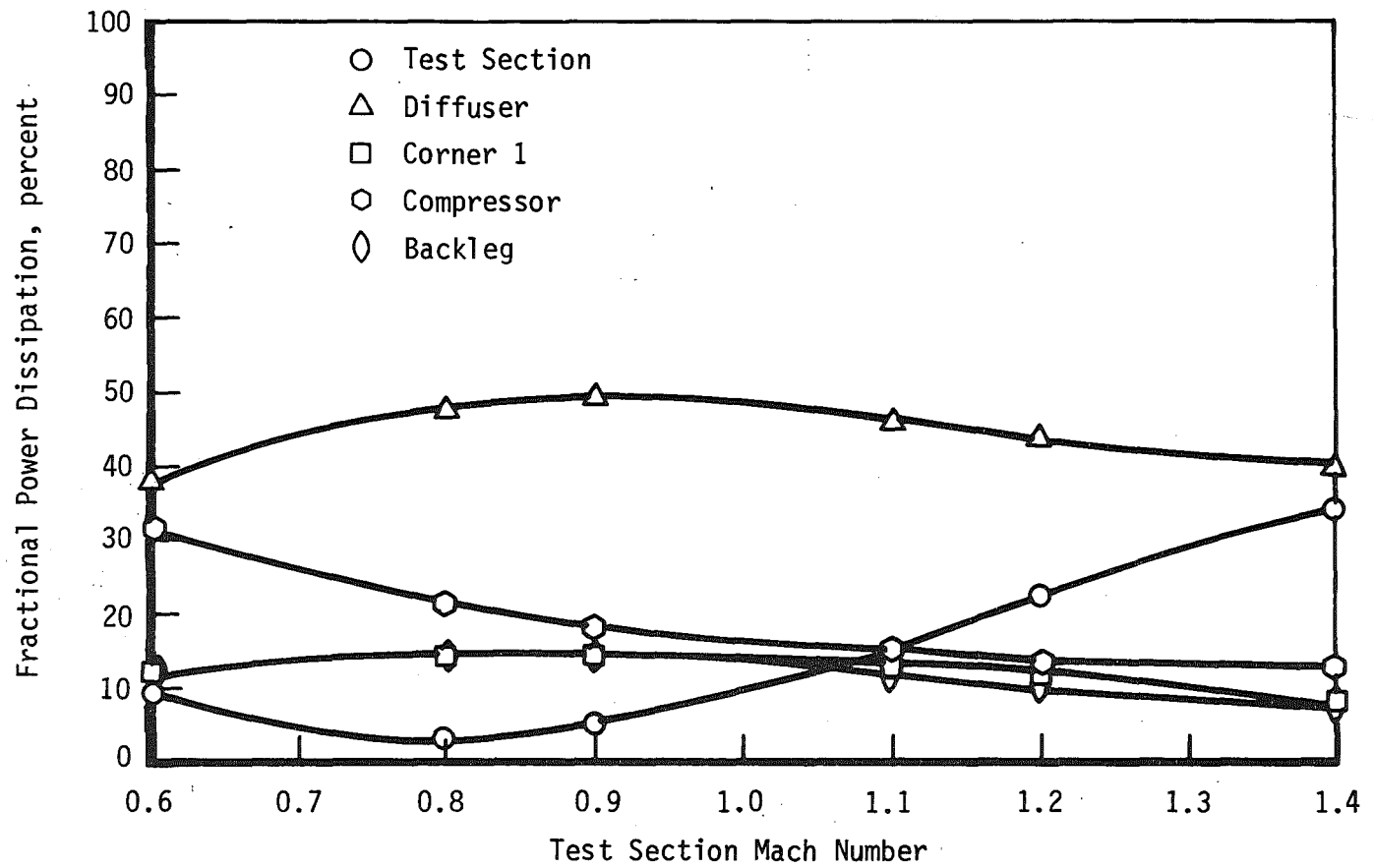
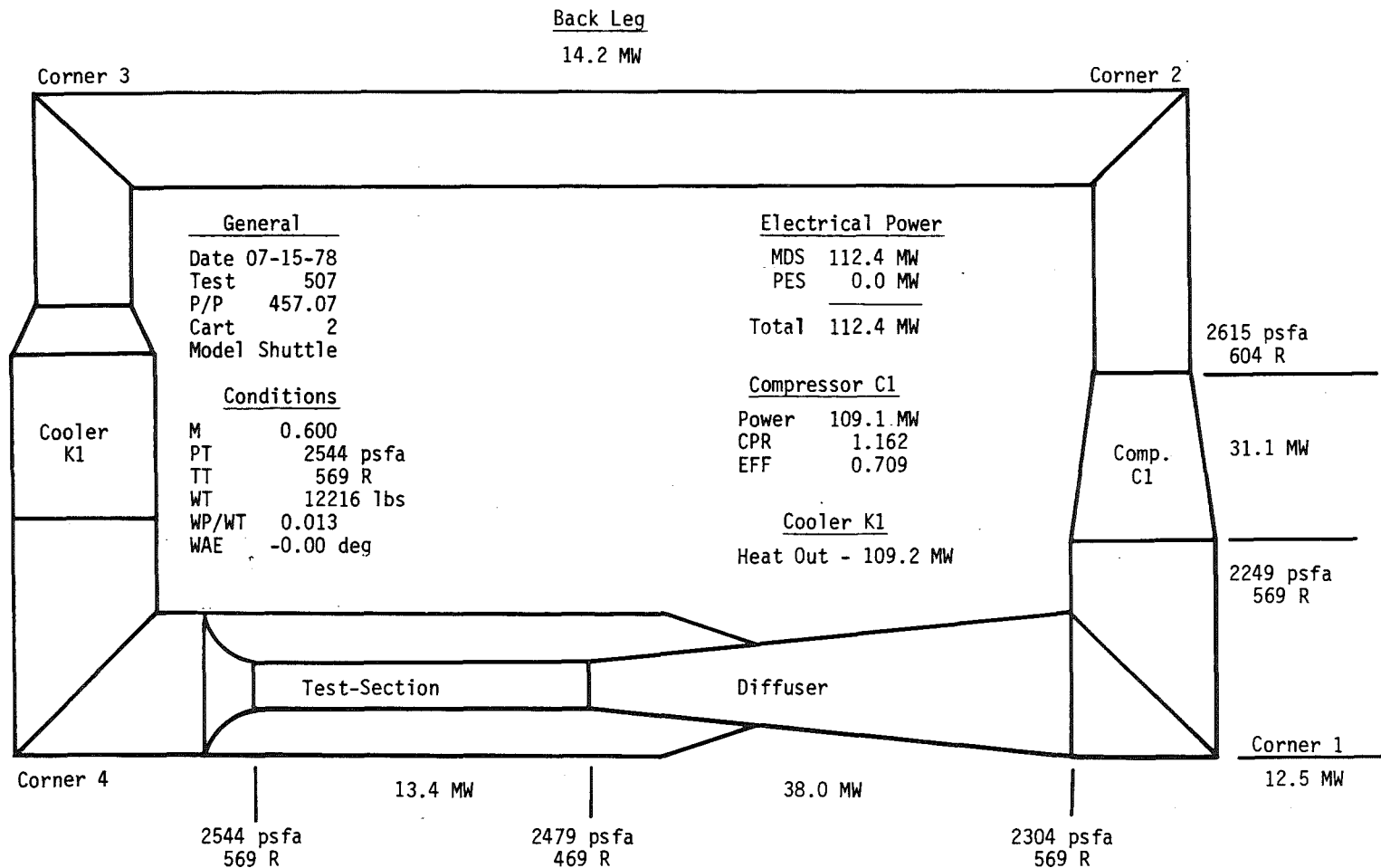


Figure 15. Tunnel Component Pressure-Loss Coefficients with Curvefits and Curvefit Coefficients.



(a) XY Plot Format

Figure 16. Historical Program Tunnel Performance Plots.



(b) Diagrammatic Plot Format

Figure 16. Concluded.

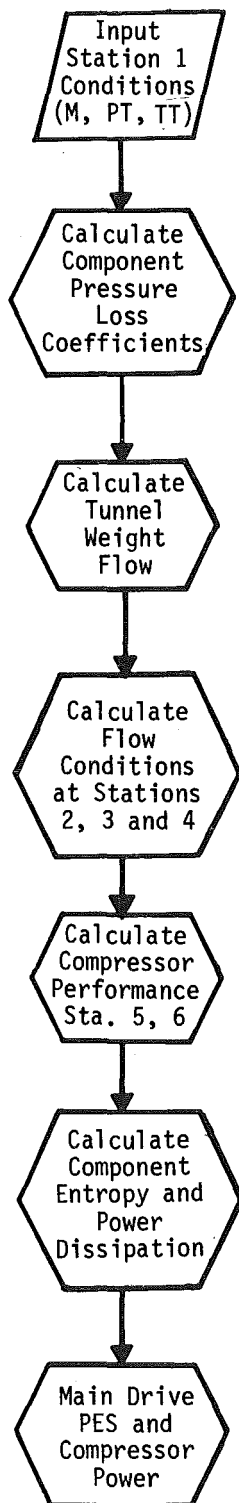


Figure 17. Analytical Model Flow Chart.

routine of the Figure 4 data to obtain the compressor efficiency, η_{comp} , at each iteration step.

Entropy change, Eq. (3-35), and power dissipation, Eq. (3-45), across each tunnel component are calculated and expressed as a percentage of the total main drive power, which is calculated using the motor efficiency information in Figure 9.

The plenum evacuation system model is used to calculate the PES configuration, Eq. (3-49), and power requirements, Eqs. (3-50) and (3-51), for each support function.

In the basic mode described here, the Analytical Model provides the same results as the Historical Program (if the same pressure-loss coefficients are used). The objective of the Analytical Model, which is to evaluate the effect of changes in the pressure losses on tunnel power, is achieved by using the model in the "ranging mode." The ranging mode utilizes the same basic logic flow shown in Figure 17; however, selected tunnel parameters may be varied or ranged in amounts selected by the user. These solutions provide the relation between variations in nearly any tunnel parameter and the main drive power requirements. The usefulness of this information will be demonstrated in Section 5.0.

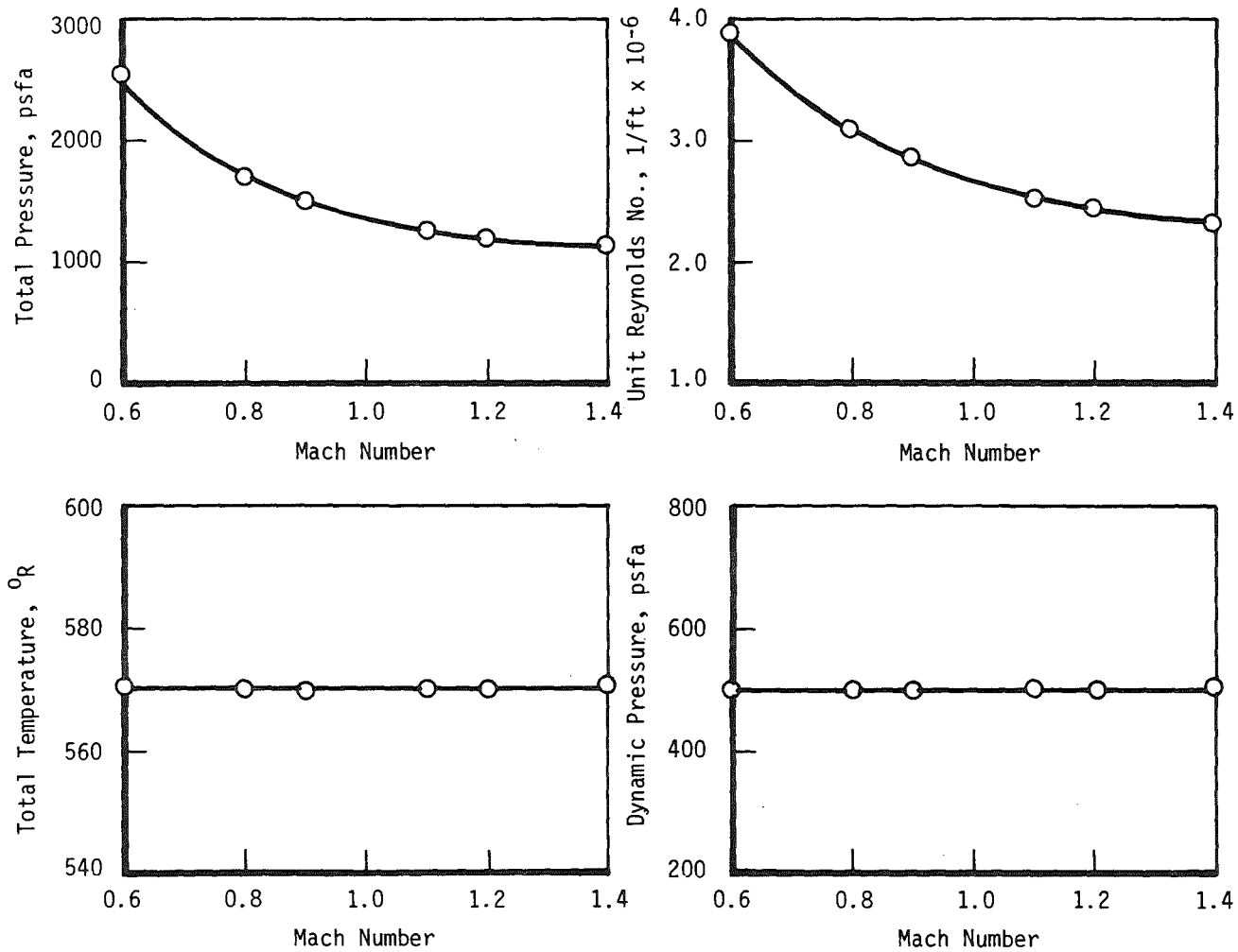
5.0 RESULTS AND DISCUSSION

5.1 General

The Tunnel 16T Historical Program was utilized for analysis of tunnel data from two Tunnel 16T test programs: a 3-percent scale model of the space shuttle orbiter and a 6-percent scale model of the F-16 fighter aircraft. Both models have a maximum cross-sectional area which produces less than 1-percent blockage in the 16T tunnel. These data are representative of a typical 16T tunnel test. The tunnel component loss coefficients from these tunnel data which were calculated using the Historical Program were then utilized as inputs to the Analytical Model.

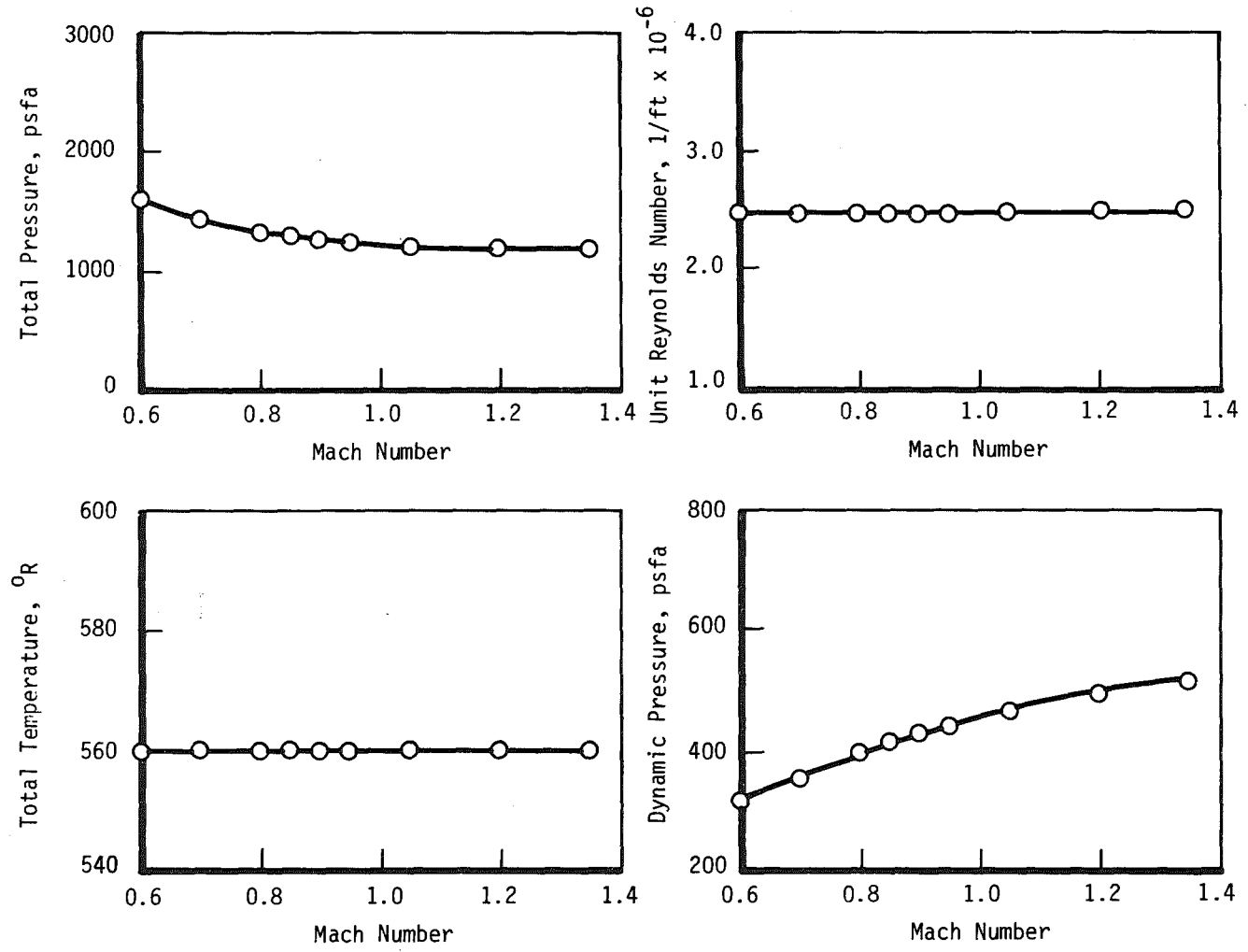
5.2 Historical Program

As a means of documenting tunnel conditions and performance, output from the Historical Program may be displayed in either an XY plot format or in a diagrammatic plot format. The ranges of tunnel test conditions (total pressure, dynamic pressure, unit Reynolds number, and total temperature) are shown versus test section inlet Mach number in Figure 18 for each of the two test data sets.



(a) NASA Shuttle Test

Figure 18. Test Conditions for Historical Program Data Sets.

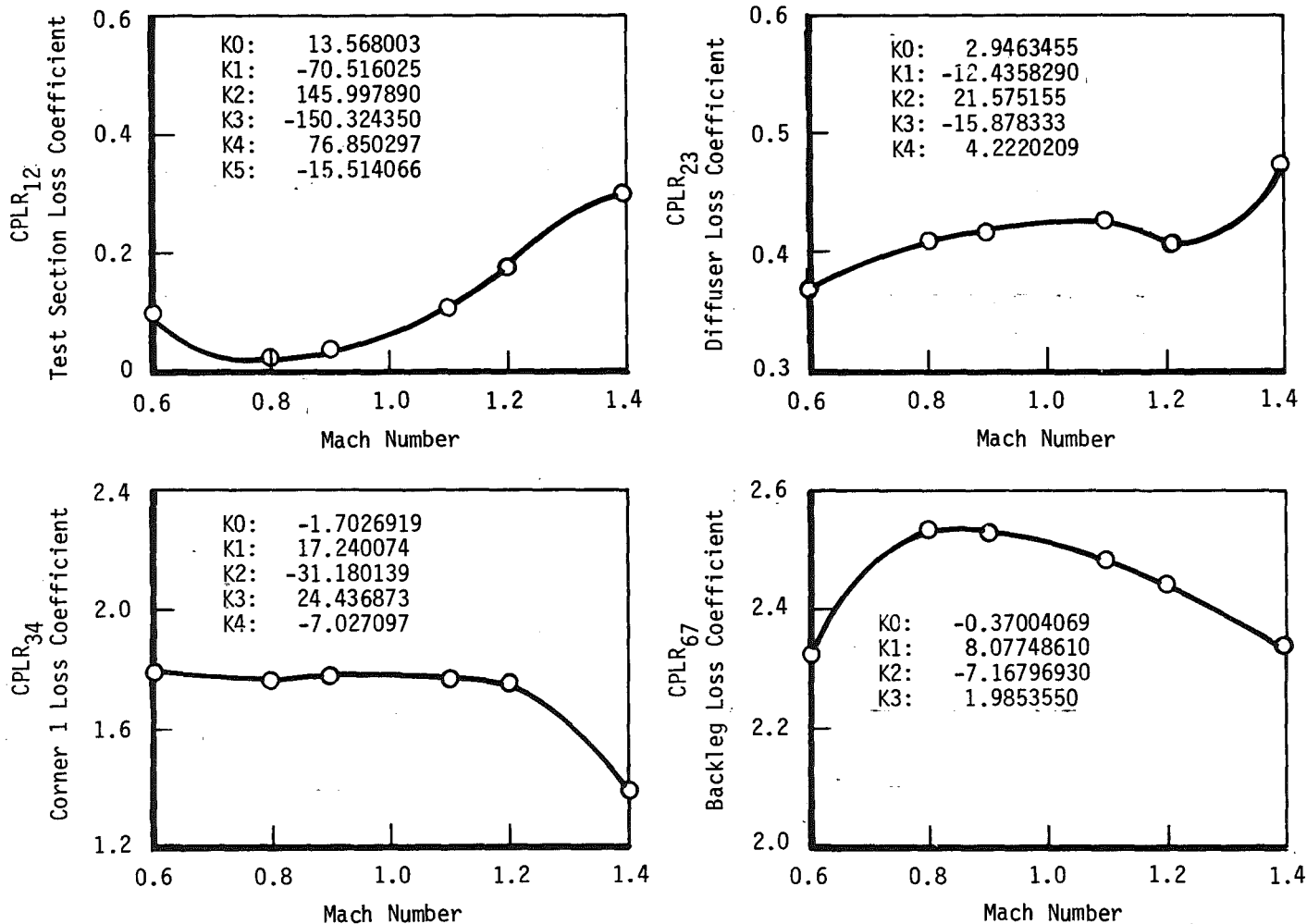


(b) F-16 Test

Figure 18. Concluded.

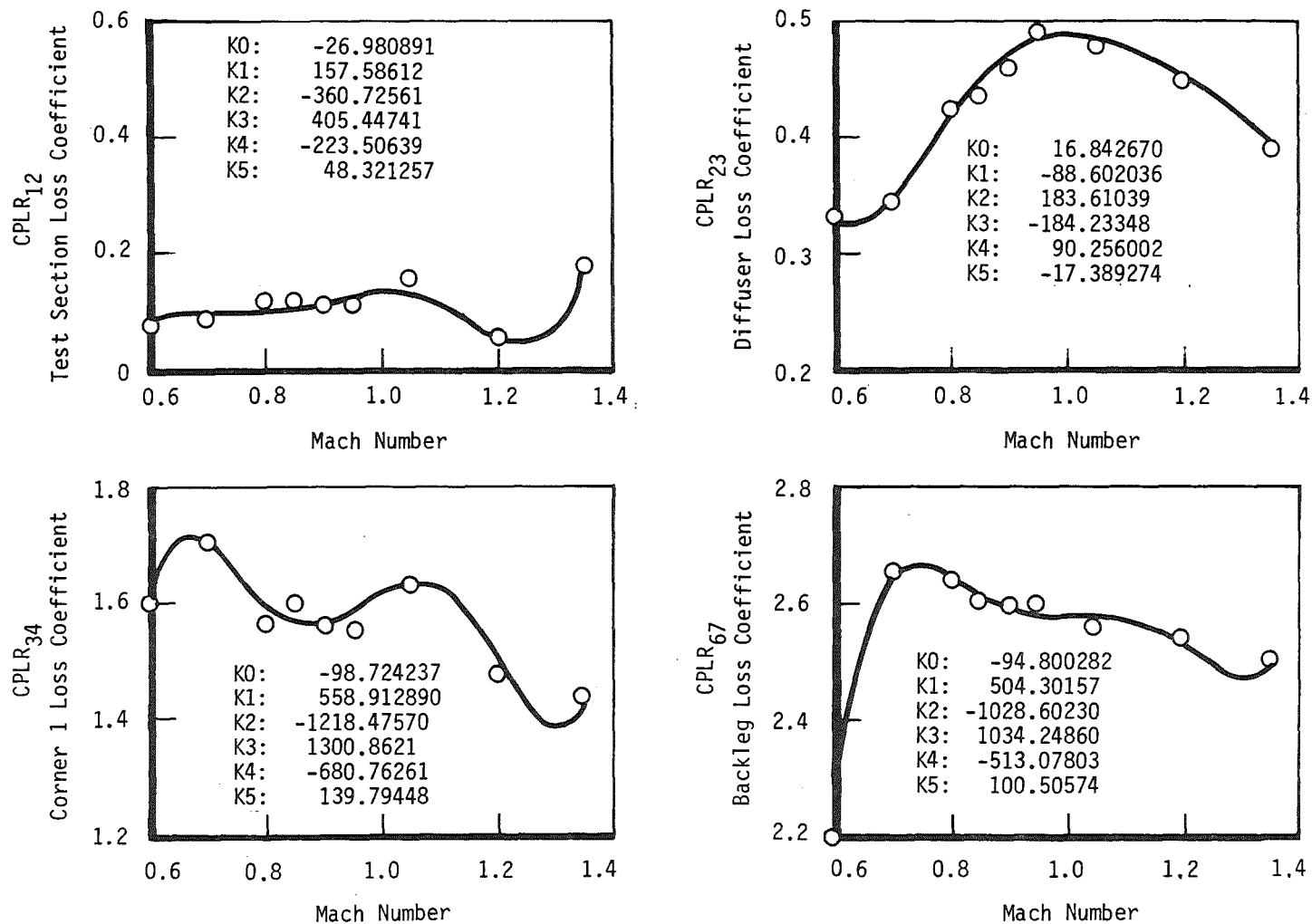
The calculated tunnel component loss coefficients are displayed in Figure 19. Significant variation is seen to exist in the loss coefficients with changing Mach number, especially in the range from $M=1.2$ to $M=1.4$. Comparison of the loss coefficients between the two sets of data shows some significant differences in the data trends; however, the magnitudes are within the same numerical ranges.

The percentage of power dissipation for each of the tunnel components is presented in Figure 20 versus test section Mach number. It is apparent that the highest percentage of losses occurs in the tunnel diffuser, which in some cases accounts for 50 percent of the tunnel main drive power requirements. The two sets of data are seen to exhibit similar magnitudes and trends of power dissipation percentages for each of the tunnel components. The tunnel compressor system accounts for a high percentage of losses at the lower Mach numbers; however, this percentage decreases as the test section Mach number increases. This trend is attributed to operation of the compressor at low pressure ratios, which are well away from the design point of the machine at the lower Mach numbers. As the Mach number and pressure ratio increase, higher compressor system efficiencies are achieved. The percentage of test section losses is comparatively low in



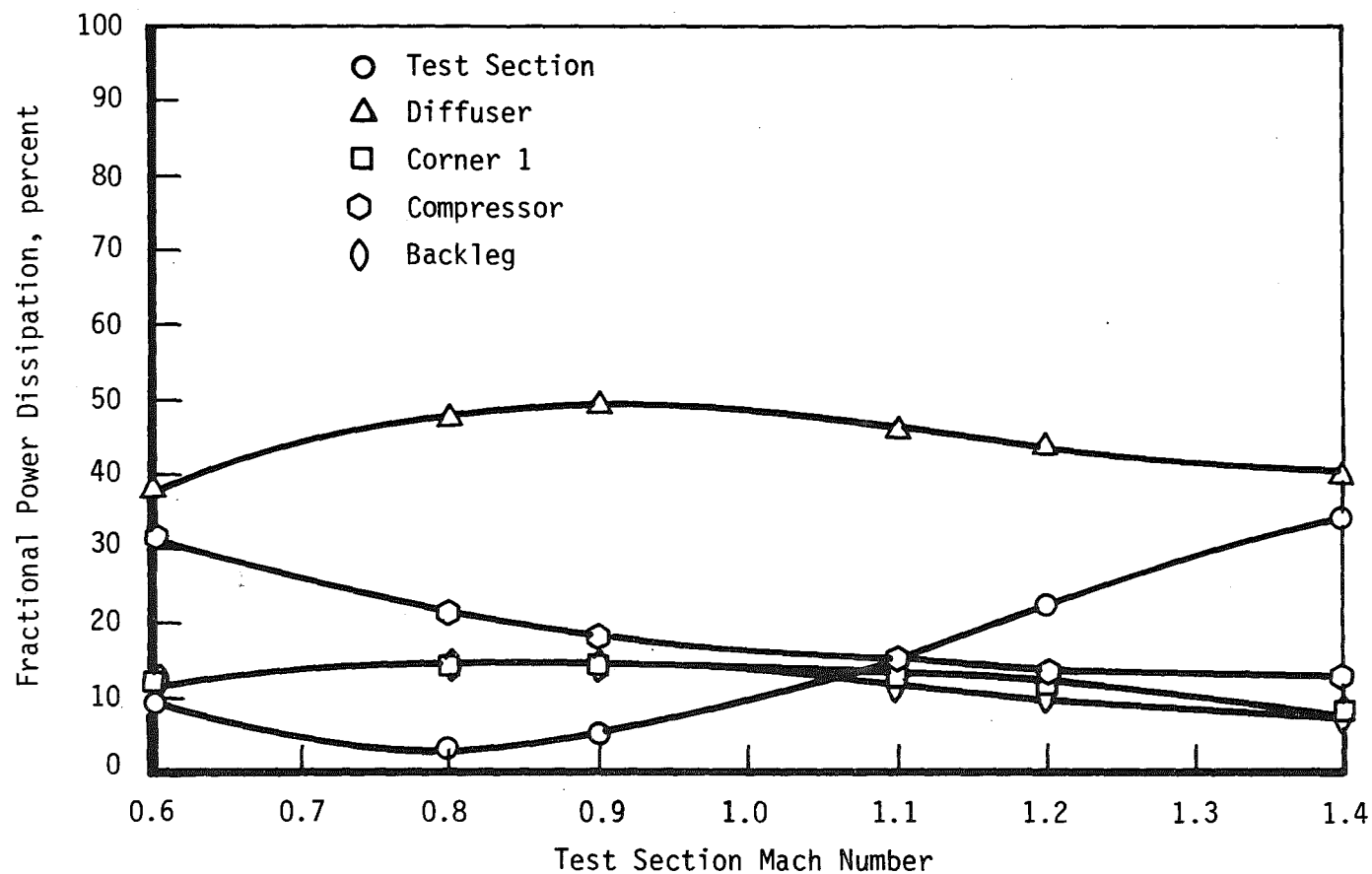
(a) NASA Shuttle Test

Figure 19. Calculated Tunnel Component Loss Coefficients.



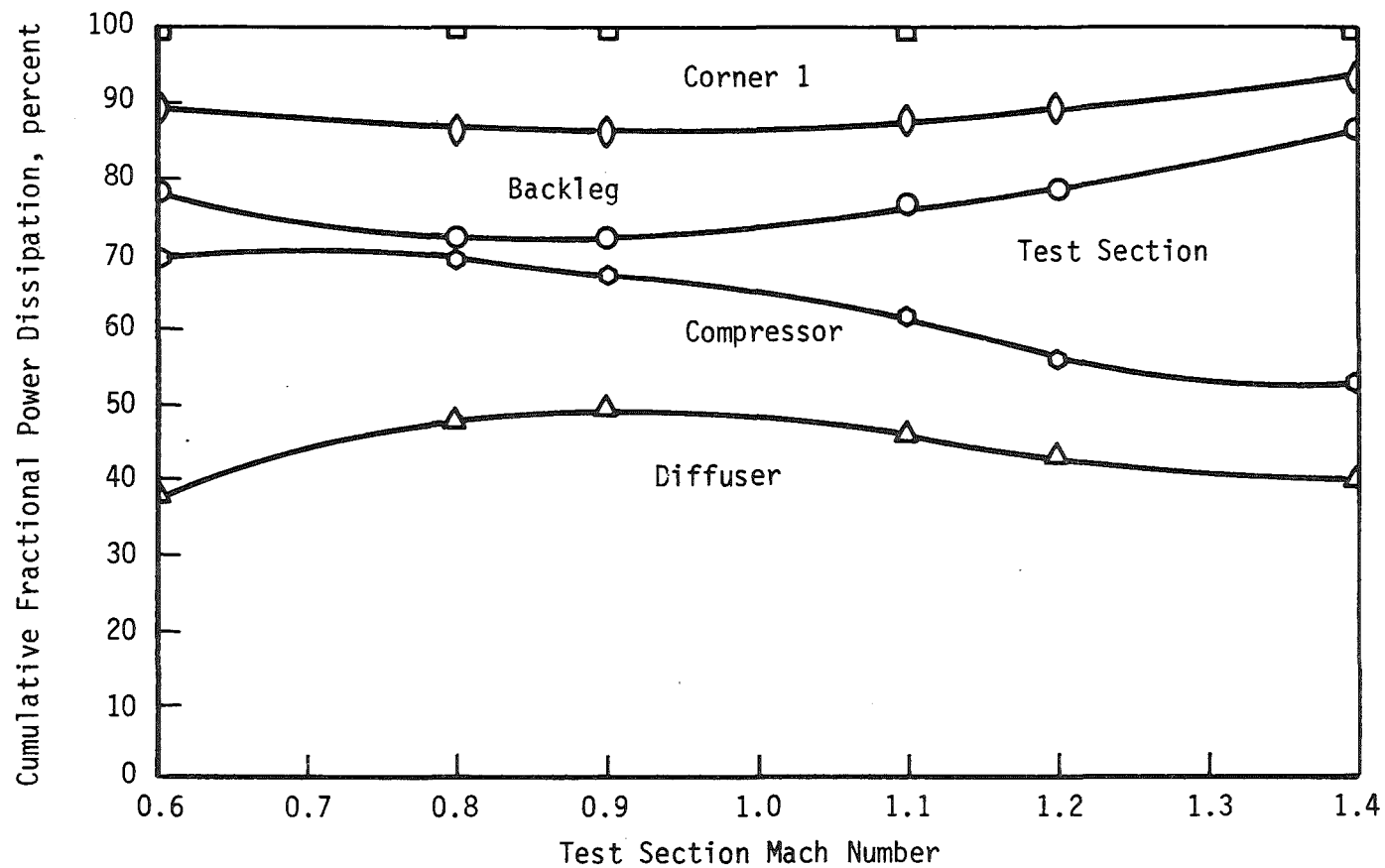
(b) F-16 Test

Figure 19. Concluded.

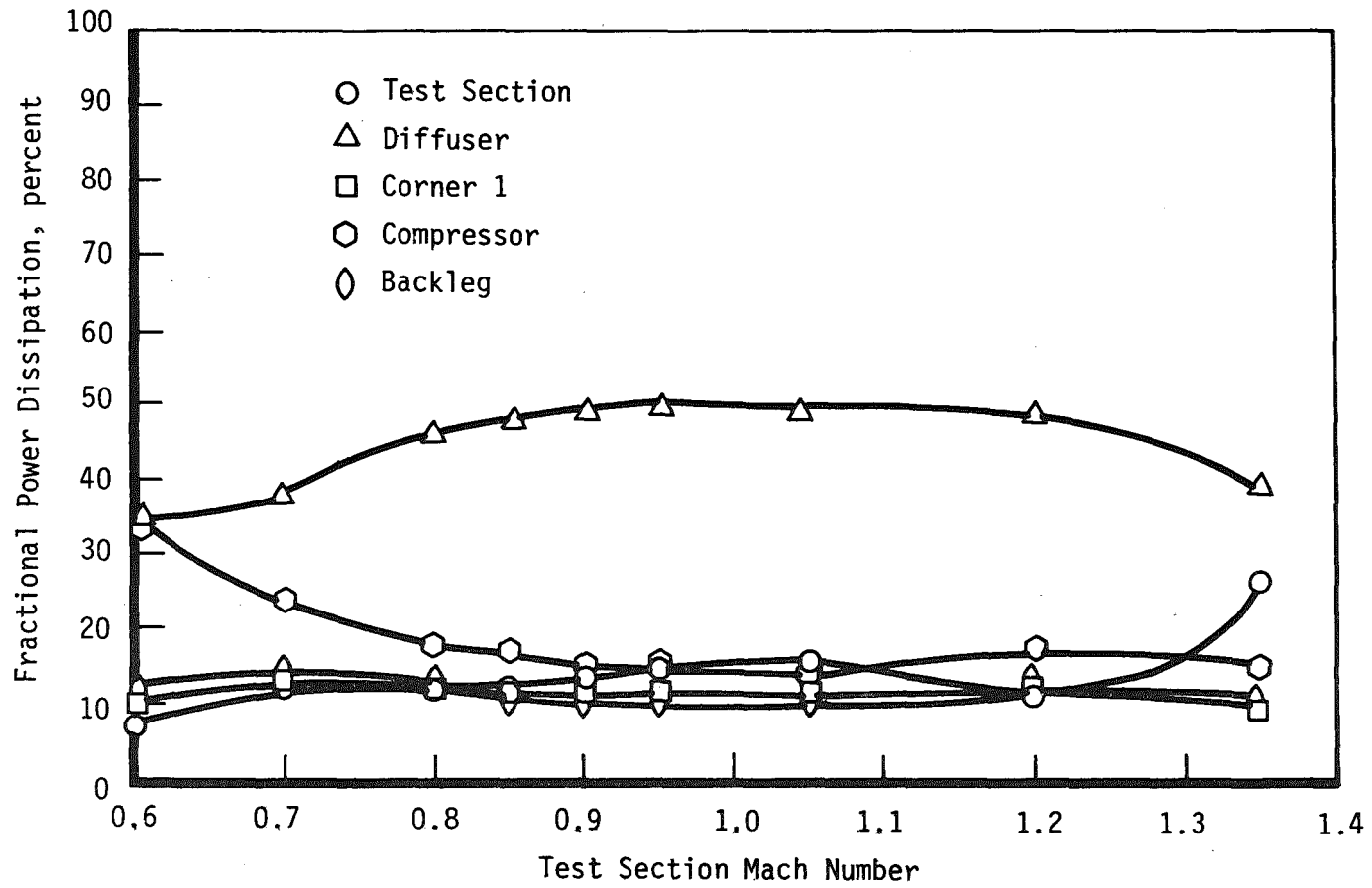


(a) NASA Shuttle Test

Figure 20. Percentage of Power Dissipation for Tunnel Components.

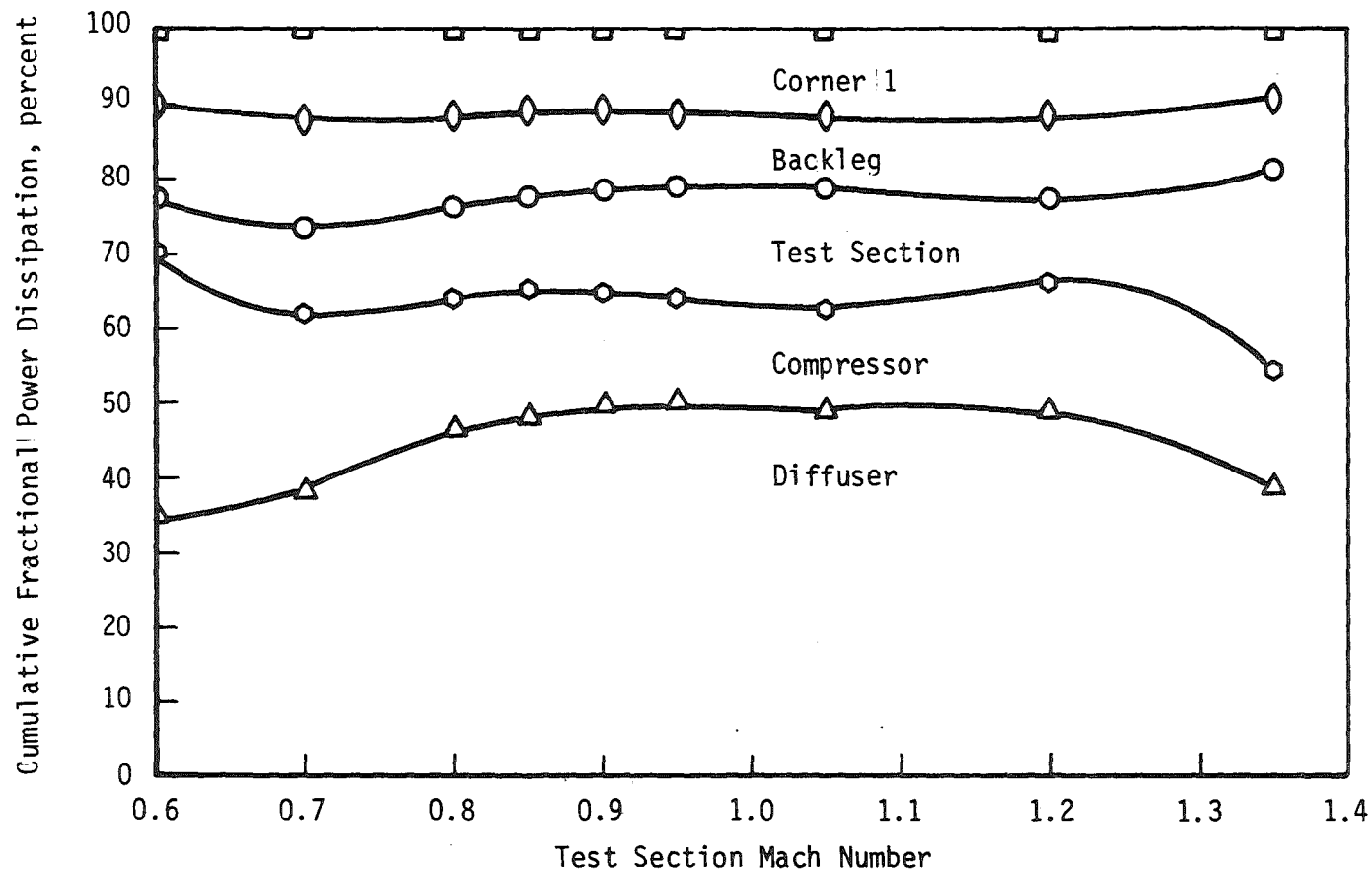


(a) Concluded
Figure 20. Continued.



(b) F-16 Test

Figure 20. Continued.



(b) Concluded
Figure 20. Concluded.

the subsonic regime, but increases substantially at the higher end of the Mach number range. It is expected that the increase is a result of a normal shock located at the exit of the test section, rather than at the diffuser entrance for these conditions. The tailing off of the diffuser losses at this point would support this hypothesis. Losses in the backleg and corner 1 components appear to be relatively independent of the test section Mach number. Combined losses in these sections consistently account for between 20 and 30 percent of the total.

The main drive power for each of the two test data sets is shown versus the test section Mach number in Figure 21. Variations in the main drive power in the two data sets are attributed to the changes in total pressure with Mach number to obtain constant dynamic pressure and unit Reynolds number, respectively.

Further presentation of Historical Program data will be included in the next section of the Analytical Model results and discussion.

5.3 Analytical Model

Comparisons of the Analytical Model and Historical Program results for identical test conditions and loss coefficients provide validations of the Analytical Model. In Table 5, a comparison of component power dissipation

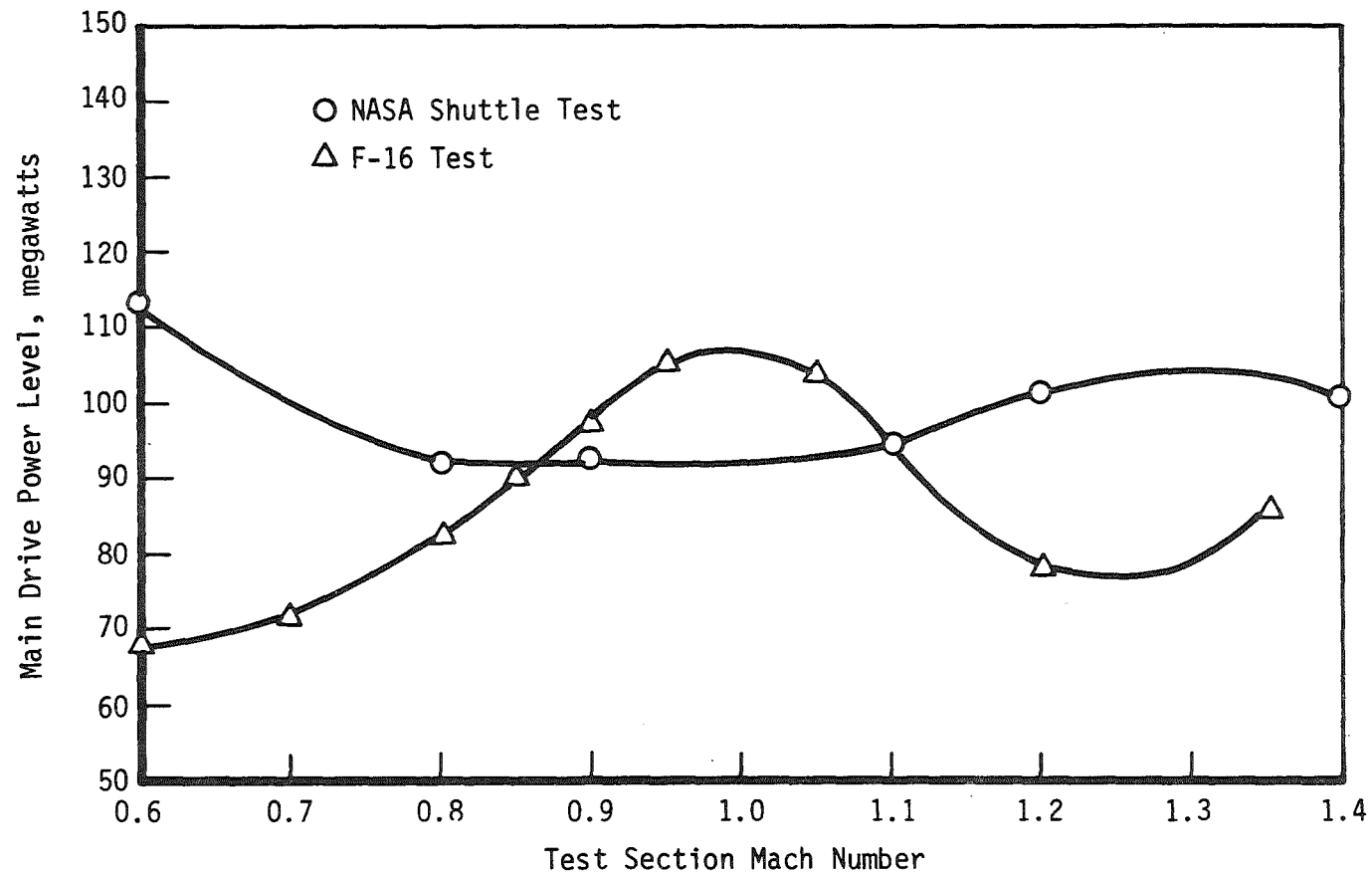


Figure 21. Main Drive Power Levels for Historical Program Data Sets.

Table 5. Power Dissipation Values for Tunnel Components
Historical Program and Analytical Model

Mach No.	Model	Power Dissipation--Megawatts					
		Test Sect.	Diff.	Corner 1	Comp. Cl	Backleg	Total
0.60	H	13.4	38.0	12.5	32.6	12.7	109.2
	A	13.4	36.4	12.4	33.9	12.7	108.8
0.80	H	1.7	43.1	12.5	21.9	14.1	93.3
	A	1.6	43.6	12.5	18.4	14.1	90.2
0.90	H	4.4	42.3	13.1	19.9	13.8	93.5
	A	4.4	43.7	13.2	16.4	13.7	91.4
1.10	H	11.6	43.5	11.5	18.4	11.4	96.4
	A	11.6	44.0	11.6	13.4	11.3	91.9
1.20	H	23.5	40.8	12.1	17.4	10.6	104.4
	A	23.5	39.5	11.9	12.6	10.5	98.0
1.40	H	36.2	46.2	8.2	16.9	7.9	115.4
	A	36.2	44.0	8.0	12.8	7.9	108.9

P. 4

values shows very good agreement for the test section, diffuser, corner 1, and backleg components. Differences in the power dissipation of the compressor system account for nearly all of the discrepancy in total shaft power between the two programs. The compressor system efficiency is a rather difficult parameter to assess in the Analytical Model, especially for operation at inlet temperatures other than the design temperature of 120°F where the fan-law corrections are applied. Examination of lines of constant efficiency in the Figure 4 compressor map gives an indication of the nonlinear nature of the compressor efficiency along a given nozzle contour resistance line. Errors in the Analytical Model table-look-up routine coupled with the empirical fan-law corrections are the source of the compressor power dissipation disagreement. The maximum deviation in total shaft power for the Analytical Model is 6 percent, which is well within the 10-percent accuracy required for this model.

A comparison of plenum evacuation system configuration and power for the Mach number range from 0.60 to 1.40 between the Historical Program and the Analytical Model is presented in Table 6. Overall, the results show reasonably good agreement in both power and compressor configurations (Eq. (3-44)) between the

Table 6. Comparison of Historical Program
and Analytical Model PES Power
and Configurations

Mach No.	Suction Flow Ratio	Model	PES Power (MW)	PES Configuration	
				Suction Flow	Pressure Cont.
0.60	0.000	Historical	18.0	--	1.11
		Analytical	10.5	--	1.11
0.80	0.038	Historical	28.0	1.12	1.21
		Analytical	28.2	1.13	1.21
0.90	0.036	Historical	30.0	1.12	1.11
		Analytical	32.7	1.13	1.11
1.10	0.035	Historical	28.0	1.12	1.11
		Analytical	26.3	1.13	1.11
1.20	0.046	Historical	32.0	1.14	1.21
		Analytical	38.7	1.15	1.21
1.40	0.035	Historical	26.0	1.14	1.21
		Analytical	26.4	1.14	1.21

tunnel data (Historical Program) and the PES model in the Analytical Model. At $M=0.60$, the Analytical Model PES power determination is significantly lower than the actual PES power. This result is attributed to PES compressors being put on unit bypass for use in establishing suction flow at the next test condition. No consideration is made in the model to allow for this situation. The suction flow configurations assigned in the Analytical Model are typically one compressor higher than the actual configuration. This is caused by the use of 4,500 cfs as the constant volume flow per compressor when actually the compressor can maintain up to 5,200 cfs, depending on the inlet-guide-vane setting and the machine pressure ratio (Figure 12). Continued use of 4,500 cfs will ensure that the assigned suction flow configurations will be capable of pumping the required plenum flows.

As previously stated, the primary function of the Analytical Model is to evaluate the effect of tunnel modifications, which change the total pressure losses across one or more tunnel components, on the tunnel power requirements. The magnitude of the change in pressure-loss coefficient for the tunnel component must be known or assumed.

The effects of reductions in the test section losses on the main drive system power are shown in Figure 22. Utilizing the component pressure coefficients given in Figure 15a, the Analytical Model produces the upper curve in Figure 22. This operating condition is termed the 100-percent case. Reducing the test section pressure-loss coefficient by 10 percent produces the middle curve, while reducing the pressure-loss coefficient by 20 percent yields the lower curve. It is apparent from this result that the reduction of losses in the test section has little effect on the tunnel power except at the upper end of the supersonic Mach number range. One would expect that, in the other direction, increases in the loss coefficient of the test section would have a pronounced effect only at the higher Mach numbers.

Reduction of the pressure loss across the tunnel diffuser produces the effect on tunnel power shown in Figure 23. The curves represent 100, 90, and 80 percent of the diffuser pressure-loss coefficient. Significant decreases in the main drive power are achieved throughout the Mach number range, thereby indicating that a small increase in the diffuser total pressure recovery will result in substantial power savings.

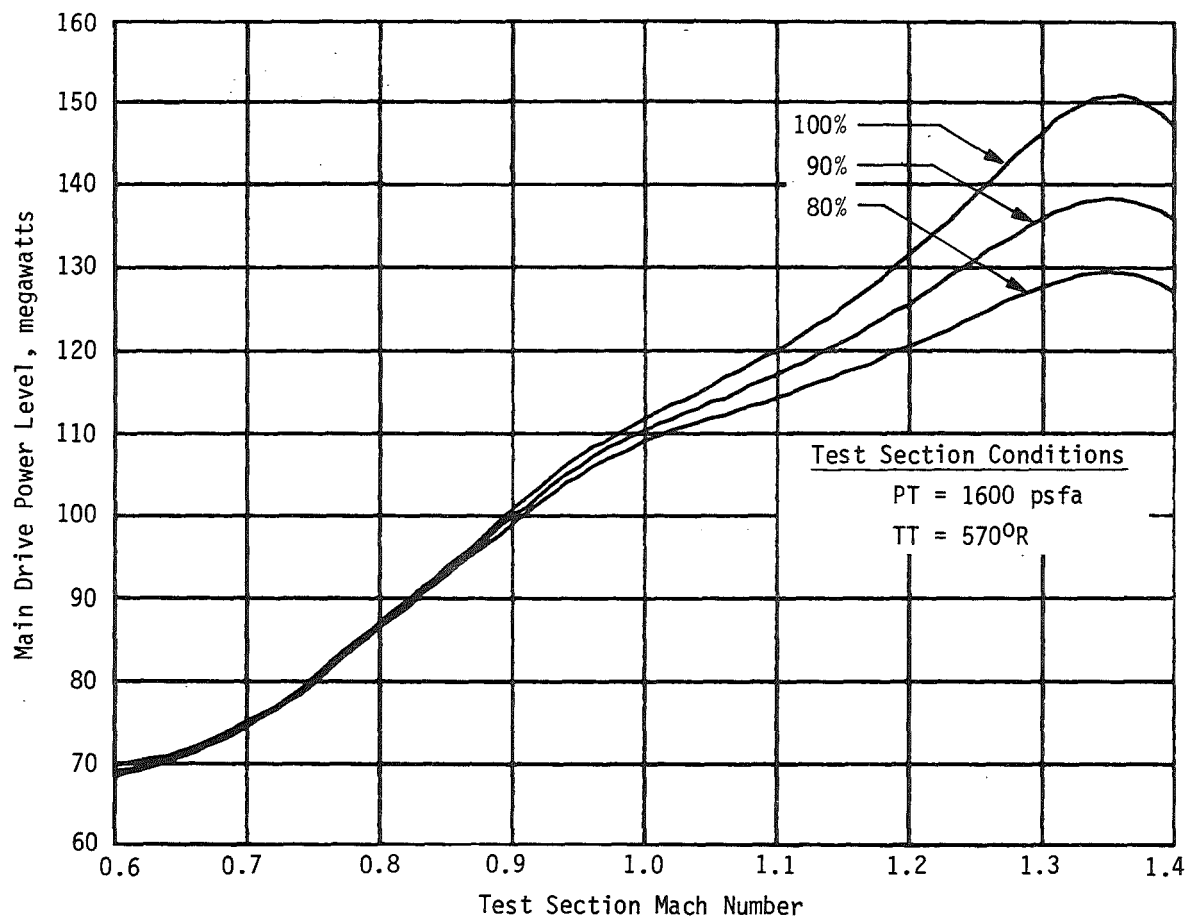


Figure 22. Effect of Variation of Test Section Pressure-Loss Coefficient on Main Drive Power.

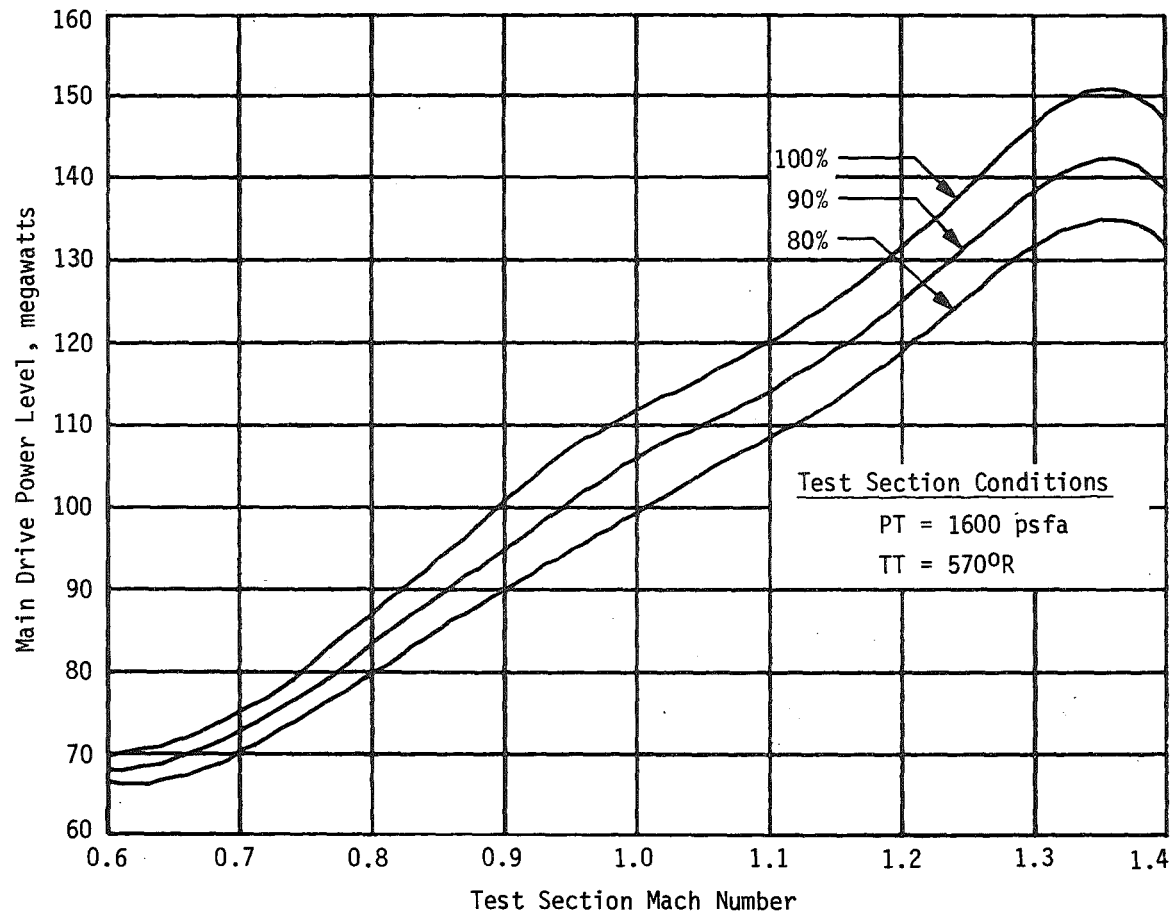


Figure 23. Effect of Variation of Diffuser Pressure-Loss Coefficient on Main Drive Power.

The effects of 10- and 20-percent reductions in the pressure-loss coefficients for the corner 1 and backleg components are illustrated in Figures 24 and 25, respectively. Although the decreases in power associated with the reduced losses are nearly constant with increasing Mach number, the magnitudes are relatively small. Modifications to these components to reduce pressure losses would, therefore, probably not be cost effective.

Increases in the C1 compressor efficiency of 1 and 2 percent have the effect on the tunnel main drive power as shown in Figure 26. Modifications to the compressor such as decreasing the rotor-to-stator seal clearances or further optimization of the stator blade settings may produce efficiency increases of the order shown in this figure. The changes in the compressor efficiency produce only small decreases in the tunnel power.

Application of the Tunnel 16T mathematical model is demonstrated in the following example for a modification to the tunnel diffuser which is to be completed in 1984. Based on a model diffuser study of potential improvements, which was conducted in the Aerodynamic Wind Tunnel (1T), it was recommended that the existing compressor protective screen be redesigned and relocated to a lower velocity region in the diffuser. Measurements

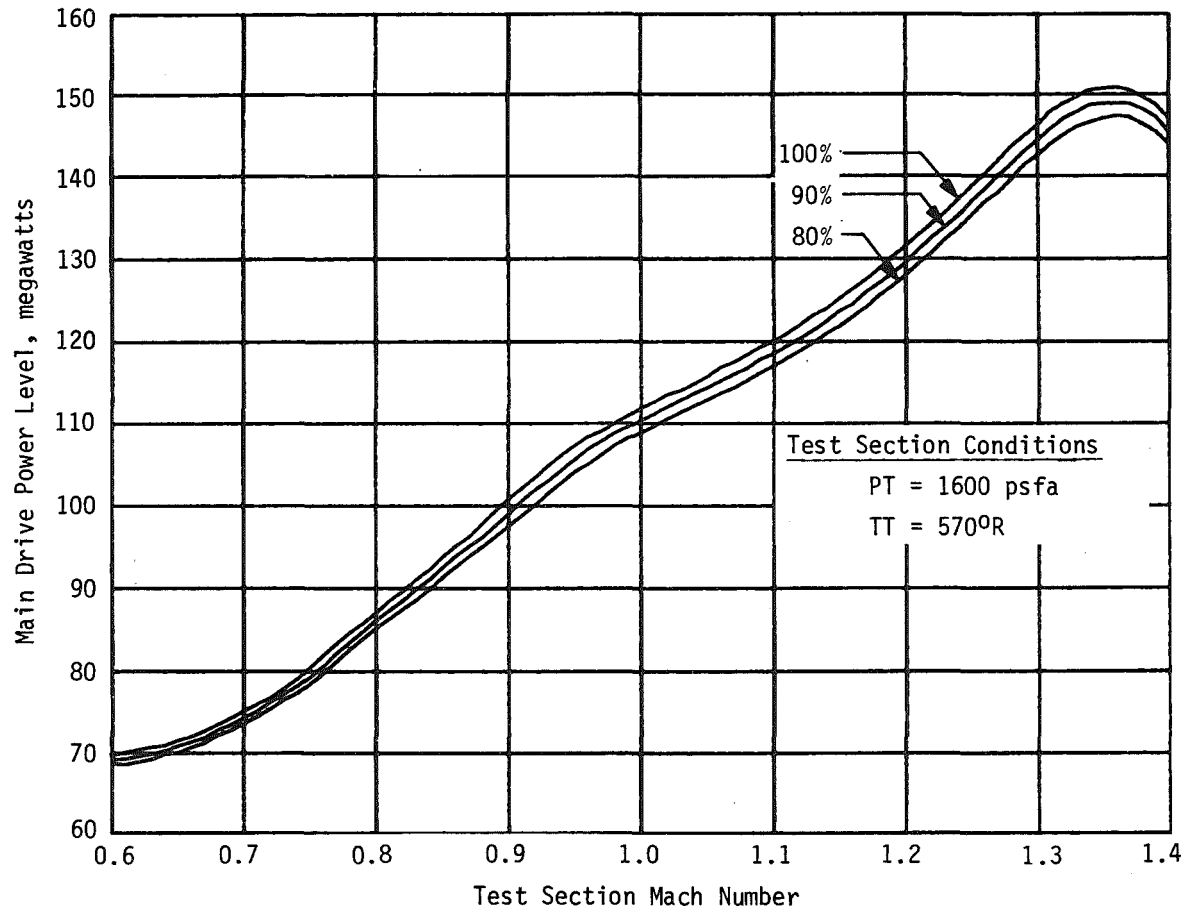


Figure 24. Effect of Variation of Corner 1 Pressure-Loss Coefficient on Main Drive Power.

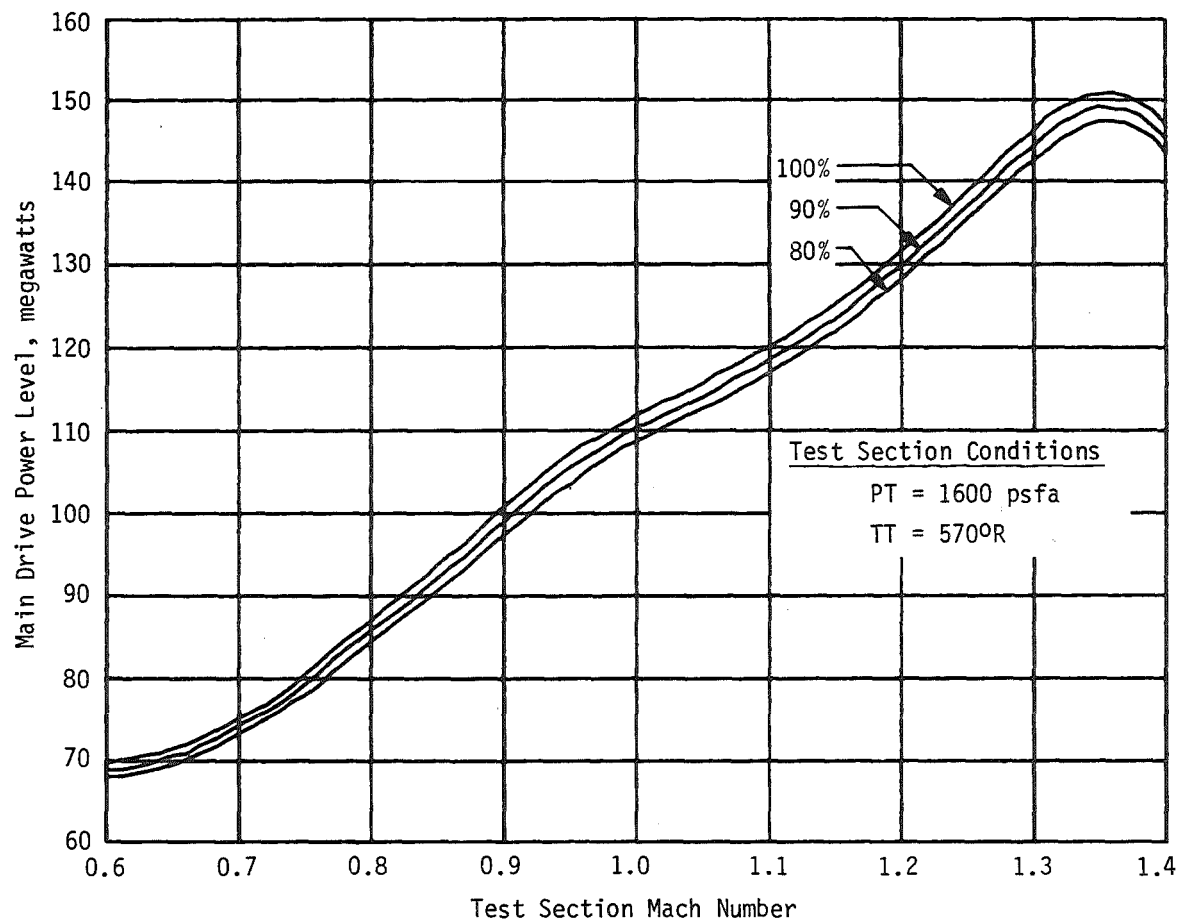


Figure 25. Effect of Variation of Backleg Pressure-Loss Coefficient on Main Drive Power.

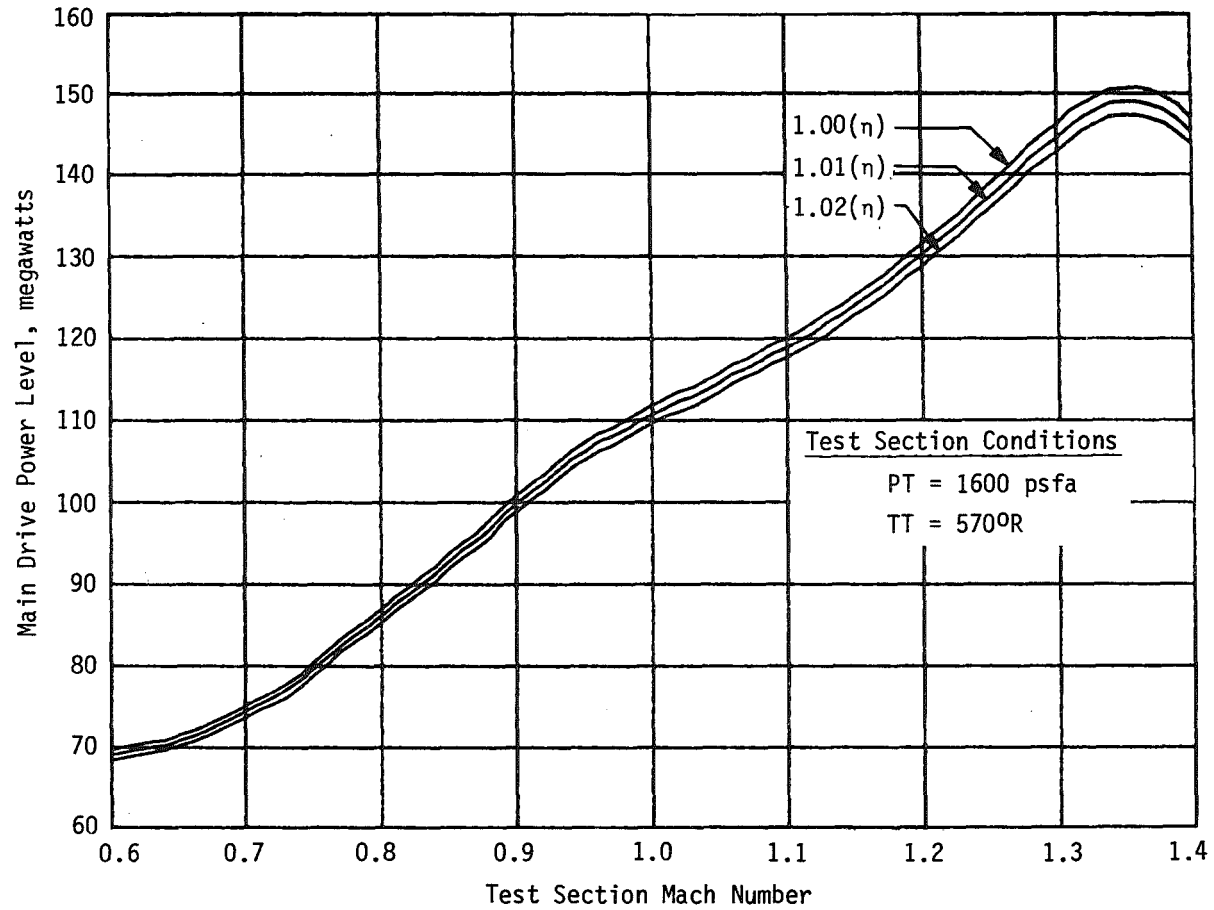


Figure 26. Effect of Variation of Compressor Efficiency on Main Drive Power.

indicated that a 2.5-percent increase in the diffuser total pressure recovery would result from implementation of this improvement.

Utilizing the Tunnel 16T Analytical Model, the impact of increased diffuser recovery on the main drive power was evaluated. For the typical test conditions of $PT=1,600$ psfa and $TT=570^{\circ}R$, the change in main drive power for a 2.5-percent increase in the diffuser total pressure recovery is shown in Figure 27.

In order to project the savings of the main drive power resulting from the screen modification to an annual savings of energy, historical records of Tunnel 16T air-on time at the various Mach numbers are required. This information is presented in Figure 28 in the form of a histogram, which was formulated using tunnel records from the past five years. By multiplying the percentage of main drive power savings with the historical percentage of air-on time for each Mach number and summing over the Mach number range, the average percent power savings is found. In this manner, the power savings for the diffuser screen modification is found to be 9.7 percent. Extrapolation of the savings was required for $0.2 < M < 0.6$ and $M=1.5$ because of insufficient data. For the average annual main drive electrical energy usage of 100,000 MW-hr, this represents

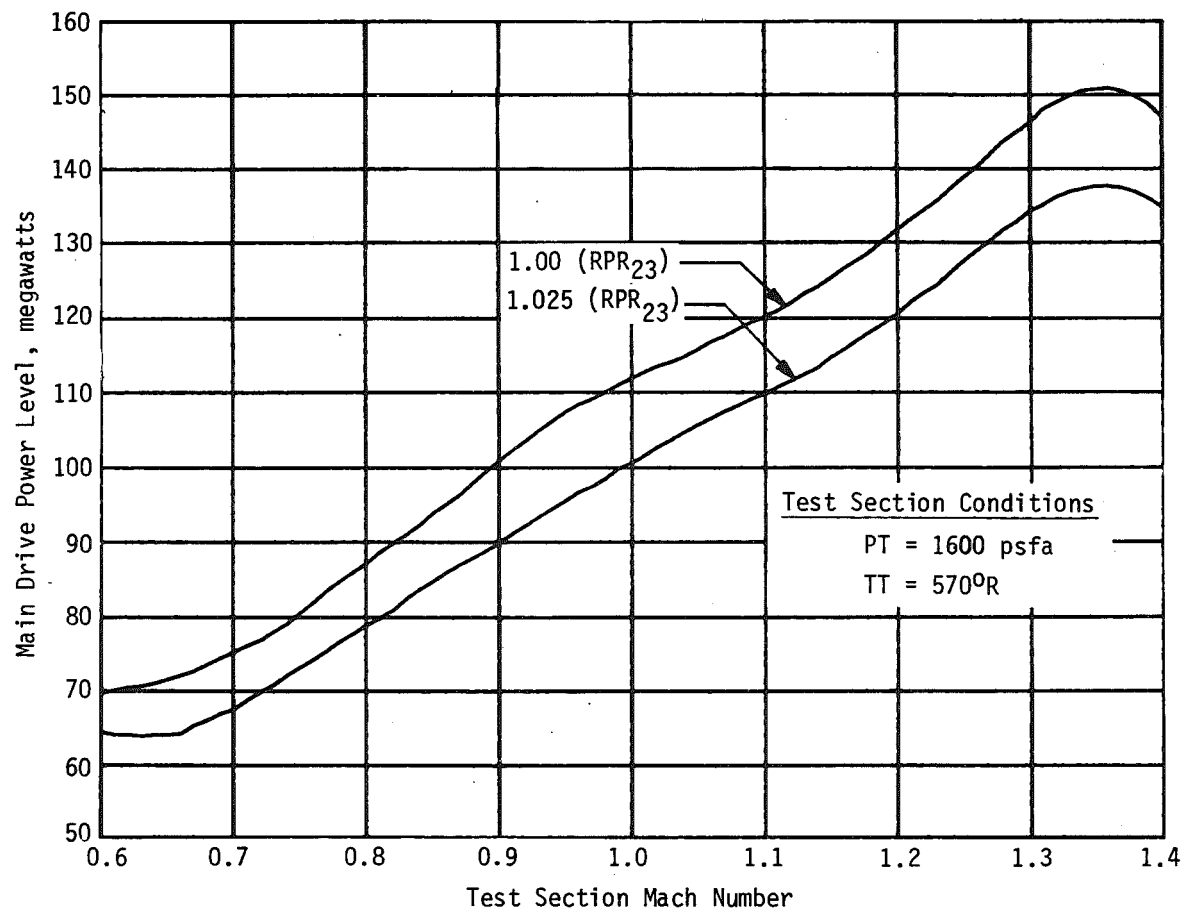


Figure 27. Effect of a 2.5-percent Increase in Diffuser Recovery on Main Drive Power.

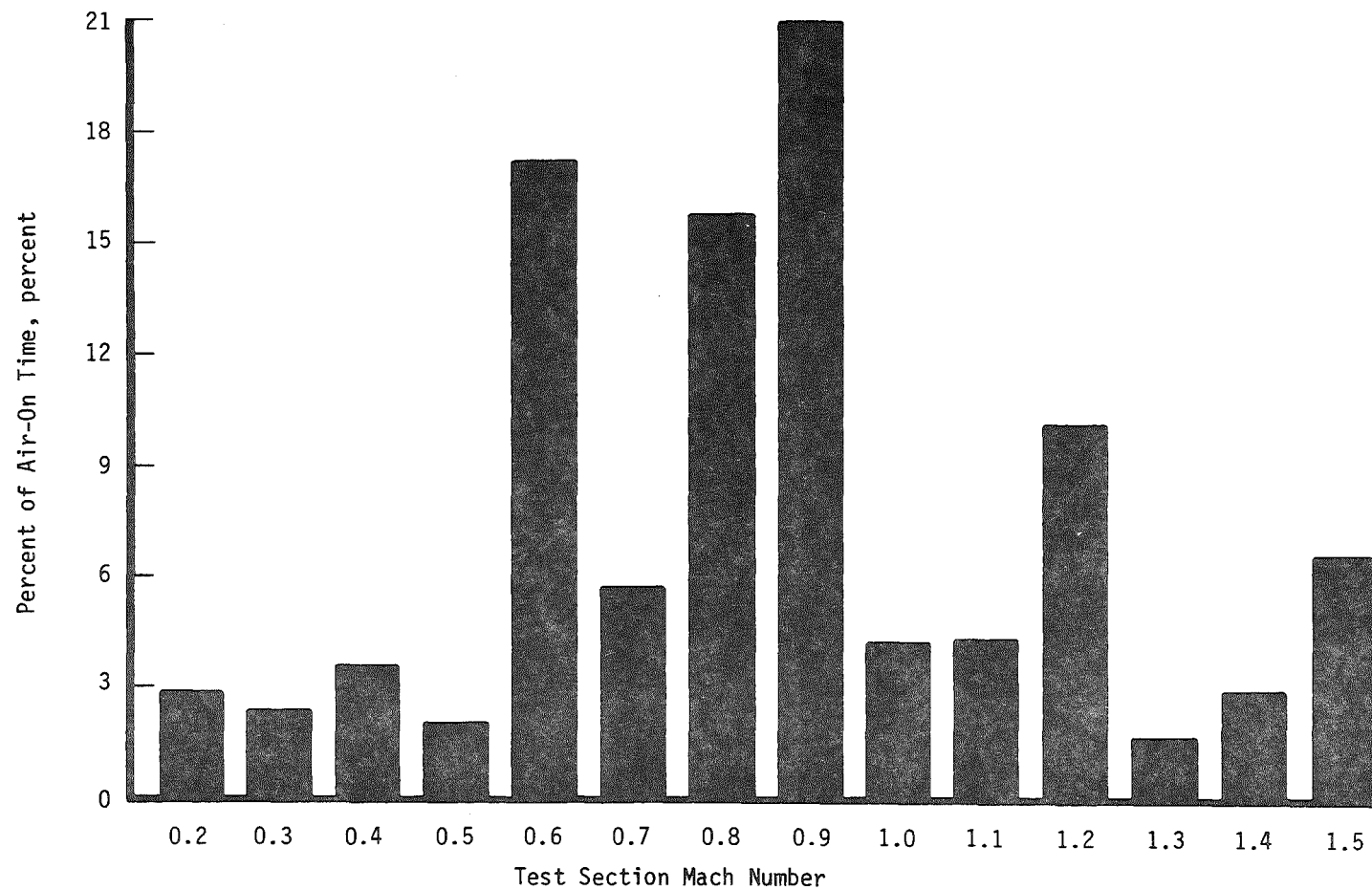


Figure 28. Historical Distribution of Air-On Test Time at Various Mach Numbers in Tunnel 16T.

an annual savings of 9,700 MW-hr. Using this result, an effective annual dollar cost savings and payback period can be established, which at current energy rates, represents an annual cost savings of \$600,000.

6.0 CONCLUSIONS AND RECOMMENDATIONS

The objective of this study was to develop and validate a mathematical model of the PWT 16-ft Propulsion Wind Tunnel (16T) which could be utilized to evaluate the tunnel performance and assess the effects of potential tunnel modifications on the main drive power requirements. The empirically based model uses existing tunnel instrumentation to evaluate tunnel component performance and to establish a data base for component pressure-loss coefficients. From the comparisons of the tunnel Analytical Model results with historic tunnel data, it is concluded that the model gives satisfactory results.

Assessment of potential pressure-loss reductions in the tunnel indicates that the tunnel component which will produce the most significant energy savings is the diffuser. Results indicate that, on the average, the tunnel power will be decreased by about 4 percent for each 1-percent increase in diffuser recovery. Less significant savings can be realized for improvements in the other tunnel components.

To improve the Analytical Model, the evaluation of compressor efficiency should be improved. This may lead to much closer agreement between the tunnel model and historic tunnel power data.

Finally, the Historical Program should be extended to allow for on-line analysis of tunnel performance. Once accomplished, the on-line model could be used to aid tunnel operators in efficient tunnel operation.

REFERENCES

1. Wattendorf, F. L. "Factors Influencing the Energy Ratio of Return Flow Wind Tunnels." Paper presented at the Fifth International Congress of Applied Mechanics, Cambridge, Massachusetts, 1938.
2. Aerospace Applied Thermodynamics Manual. New York: Society of Automotive Engineers, 1962.
3. Jackson, F. M. "A Methodology for Evaluating Ducting Pressure Losses in Aerospace Test Facilities," Arnold Engineering Development Center CW-01-6-76, Arnold Air Force Station, Tennessee, June 1976.
4. Test Facilities Handbook. Eleventh edition. Vol. 4. Arnold Air Force Station, Tennessee: Arnold Engineering Development Center, 1981.
5. Estabrooks, B. B., and J. R. Millilo. "Aerodynamic Performance of the AEDC-PWT Transonic Circuit Compressor," Arnold Engineering Development Center TR-57-15, Arnold Air Force Station, Tennessee, October 1957.
6. Parli, C. L. "Aerodynamic Calibration of the AEDC 16-ft Transonic Tunnel Compressor with Fiberglass Rotor Blades," Arnold Engineering Development Center TR-65-242, Arnold Air Force Station, Tennessee, November 1965.
7. Faires, Virgil M. Thermodynamics. Fifth edition. New York: Macmillan Publishing Company, Inc., 1970.

APPENDIX A

DERIVATION OF FAN-LAW CORRECTIONS FOR
COMPRESSOR C1

As a means of correcting the performance parameters for compressor C1 to reference conditions, scaling laws are utilized which were derived from the so-called fan laws. Basically, the fan laws state that for a given value of the flow parameter, Q/N , the same energy addition will always result. (Note: Q is the inlet volume flow, and N is the rotational speed of the machine.) Alternately stated, if the performance of the machine at one volume flow and speed are known (condition a), then the same performance would result for another volume flow (condition b), provided that

$$N_b = \frac{Q_b}{(Q/N)_a} \quad (A-1)$$

Applying the First Law of Thermodynamics for two compressor operating points a and b, one has

$$\left\{ \frac{C_p}{\eta} T T_4^{\frac{\gamma-1}{\gamma}} [\lambda^{\frac{\gamma-1}{\gamma}} - 1] \right\}_a = \left\{ \frac{C_p}{\gamma} T T_4^{\frac{\gamma-1}{\gamma}} [\lambda^{\frac{\gamma-1}{\gamma}} - 1] \right\}_b \quad (A-2)$$

Rearranging

$$\lambda_b = \{1 + (\frac{\eta_b}{\eta_a}) (\frac{T_{T4,a}}{T_{T4,b}}) [\lambda_a^{\frac{\gamma-1}{\gamma}} - 1]^{\frac{\gamma}{\gamma-1}}\} \quad (A-3)$$

For operation at constant Q/N , assume $\eta_b/\eta_a = 1.0$.

Equation (A-3) becomes

$$\eta_b = \{1 + (\frac{T_{T4,a}}{T_{T4,b}}) [\lambda_a^{\frac{\gamma-1}{\gamma}} - 1]^{\frac{\gamma}{\gamma-1}}\} \quad (A-4)$$

The effects of compressibility are accounted for by introducing the approximate relation

$$(\frac{Q}{N\lambda^{1/3}})_a = (\frac{Q}{N\lambda^{1/3}})_b \quad (A-5)$$

The $1/3$ power is a modification of the $\gamma-1/\gamma$ power. It was arrived at by including compressor efficiency effects through use of a polytropic efficiency. Using this modified relation for a constant speed operation, Eq. (A-4) is written

$$\lambda_b = \{1 + (\frac{T_{T4,a}}{T_{T4,b}}) [\lambda_a^{\frac{1}{3}} - 1]\}^{3.0} \quad (A-6)$$

For the reference state b being referred to as the corrected condition, with $T_T=580^{\circ}\text{R}$, the scaling laws used for compressor C1 are written from Eqs. (A-6) and (A-5) as

$$\lambda_c = \{1 + (\frac{T_T}{580^{\circ}\text{R}})^4 [\lambda^{\frac{1}{3}} - 1]\}^{3.0} \quad (\text{A-7})$$

$$Q_c = Q(\frac{\lambda_c}{\lambda})^{\frac{1}{3}} \quad (\text{A-8})$$

APPENDIX B

DERIVATION OF ADIABATIC EFFICIENCY EQUATION FOR A
POLYTROPIC COMPRESSION

The adiabatic efficiency for the C1 compressor is equal to the ratio of input power for the isentropic process divided by the actual (or polytropic) input power. This may be expressed in terms of total enthalpy, HT, as

$$\eta_{\text{comp}} = \frac{(HT)_5 - (HT)_4}{(HT)_6 - (HT)_4} = \frac{(CpTT)_5 - (CpTT)_4}{(CpTT)_6 - (CpTT)_4} \quad (B-1)$$

Assuming constant specific heat, Cp, with changing temperature, Eq. (B-1) is written as

$$\eta_{\text{comp}} = \frac{TT_5 - TT_4}{TT_6 - TT_4} \quad (B-2)$$

For an isentropic, ideal gas, the pressure-density relation across the compressor is given as

$$\frac{P_4}{(P_4)^\gamma} = \frac{P_5}{(P_5)^\gamma} \quad (B-3)$$

which may be rewritten as

$$(P_4)^{1-\gamma} (RT_4)^\gamma = (P_5)^{1-\gamma} (RT_5)^\gamma \quad (B-4)$$

Rearranging this equation, one has

$$\frac{T_4}{T_5} = \left(\frac{P_4}{P_5} \right)^{\frac{\gamma-1}{\gamma}} \quad (B-5)$$

which, written in terms of total conditions is

$$\frac{TT_4}{TT_5} = \left(\frac{PT_4}{PT_5} \right)^{\frac{\gamma-1}{\gamma}} \quad (B-6)$$

Combining Eqs. (B-2) and (B-6), one obtains the relation

$$\eta_{\text{comp}} = \frac{TT_4 \left(\frac{PT_5}{PT_4} \right)^{\frac{\gamma-1}{\gamma}} - TT_4}{TT_6 - TT_4} \quad (B-7)$$

Rearranging, and noting that $PT_5 = PT_6$, and $\lambda = PT_6/PT_5$, gives

$$TT_6 - TT_4 = \frac{TT_4 (\lambda^{\frac{\gamma-1}{\gamma}} - 1)}{\eta_{\text{comp}}} \quad (B-8)$$

NOMENCLATURE

A	Area, ft^2
AVL	Availability, Btu/lbm
c	Speed of sound, ft/sec
CONPES	PES compressor configuration
Cp	Specific heat at constant pressure, Btu/lbm- $^{\circ}\text{R}$
CPLR	Component pressure-loss coefficient
DP	Discharge pressure of PES compressor, psfa
F	Stream impulse function, lbf
\bar{F}	Impulse parameter
FDP	Component fractional power dissipation
g	Gravity, $\text{ft-lbm/sec}^2\text{-lbf}$
H	Cooler heat transfer, MW
HPI	Isentropic compressor shaft power, MW
HPMi	Power input to individual main drive motors, ($i=1$ to 4), MW
HPMDS	Total power input to main drive system, MW
HPP	Polytropic compressor shaft power, MW
HT	Total enthalpy, Btu/lbm
Ki	Coefficients for component pressure loss polynomials ($i=0$ to 5)
M	Mach number
MWi	Power input to PES pressure control stages, ($i=S1, S2$ and $S3$), MW
N	Compressor rotational speed, rpm

P	Static pressure, psfa
PD	Component power dissipation, MW
PDWT	Total tunnel power dissipation, MW
PR	PES compressor pressure ratio
Pri	PES stage pressure ratio (i=S1, S2, and S3)
PRPES	PES pressure control pressure ratio
PRSF	PES suction flow pressure ratio
PT	Total pressure, psfa
q	Dynamic pressure, psfa
Q	Volume flow, cfs
R	Gas constant, ft-lbf/lbm-°R
RPR	Tunnel component total pressure recovery
S	Entropy, Btu/lbm-°R
T	Static temperature, °R
TT	Total temperature, °R
T _{ds}	Dead-state temperature, °R
V	Velocity, ft/sec
W	Mass flow rate, lbm/sec
\bar{W}	Mass flow parameter
WA	Test section wall angle, deg
WP	Tunnel auxiliary mass flow rate, lbm/sec

Greek Letters

Δ	Change across tunnel component
γ	Specific heat ratio

η_{comp}	Compressor efficiency
η_{mi}	Efficiency of individual main drive motors, (i=1 to 4)
η_{mds}	Efficiency of main drive system
λ	Compressor pressure ratio
ρ	Density, lbm/ft ³

Subscripts

1	Test section inlet station
2	Diffuser inlet station
3	Corner 1 inlet station
4	Compressor inlet station
5	Compressor exit station (isentropic)
6	Compressor exit station (polytropic)
7	Backleg exit station
a	Compressor operating point
b	Compressor operating point
c	Corrected compressor conditions (TT=580°R)
x	Component inlet station
y	Component exit station